Cloning of Components of a Novel Subthreshold-Activating K$^+$ Channel with a Unique Pattern of Expression in the Cerebral Cortex

M. J. Saganich,[1] **E. Vega-Saenz de Miera,**[1] **M. S. Nadal,**[1] **H. Baker,**[4] **W. A. Coetzee,**[1,3] **and B. Rudy**[1,2]

[1]*Departments of Physiology and Neuroscience,* [2]*Biochemistry, and* [3]*Pediatric Cardiology, New York University School of Medicine, New York, New York, 10016, and* [4]*Cornell University Medical College, Burke Medical Research Institute, White Plains, New York 10605*

Potassium channels that are open at very negative membrane potentials govern the subthreshold behavior of neurons. These channels contribute to the resting potential and help regulate the degree of excitability of a neuron by affecting the impact of synaptic inputs and the threshold for action potential generation. They can have large influences on cell behavior even when present at low concentrations because few conductances are active at these voltages. We report the identification of a new K$^+$ channel pore-forming subunit of the ether-à-go-go (Eag) family, named Eag2, that expresses voltage-gated K$^+$ channels that have significant activation at voltages around -100 mV. Eag2 expresses outward-rectifying, *non-inactivating* voltage-dependent K$^+$ currents resembling those of Eag1, including a strong dependence of activation kinetics on prepulse potential. However, Eag2 currents start activating at subthreshold potentials that are 40–50 mV more negative than those reported for Eag1. Because they activate at such negative voltages and do not inactivate, Eag2 channels will contribute sustained outward currents down to the most negative membrane potentials known in neurons. Although Eag2 mRNA levels in whole brain appear to be low, they are highly concentrated in a few neuronal populations, most prominently in layer IV of the cerebral cortex. This highly restricted pattern of cortical expression is unlike that of any other potassium channel cloned to date and may indicate specific roles for this channel in cortical processing. Layer IV neurons are the main recipient of the thalamocortical input. Given their functional properties and specific distribution, Eag2 channels may play roles in the regulation of the behavioral state-dependent entry of sensory information to the cerebral cortex.

Key words: potassium channels; Eag; cerebral cortex; in situ *hybridization; molecular cloning; rat; layer IV; M currents*

Potassium channels have important functions as modulators of neuronal excitability (Llinas, 1988; McCormick, 1990; Baxter and Byrne, 1991; Hille, 1992). Their large diversity and differential cellular and subcellular neuronal expression contribute to the specific electrical behavior of distinct neurons (Llinas, 1988; Rudy, 1988; Latorre et al., 1989; McCormick, 1990; Baxter and Byrne, 1991; Hille, 1992). Moreover, because K$^+$ channels are often key targets of the second messenger cascades activated by neurotransmitters and neuropeptides (Klein et al., 1982; Kaczmareck and Levitan, 1987; Levitan, 1988; Hille, 1992), their diversity and differential neuronal expression also contribute to the specificity of neuromodulatory responses.

Of special interest are those K$^+$ channels that are open at membrane potentials below the threshold for action potential generation. These channels can contribute to the resting potential and regulate the degree of excitability of a neuron. By activating or blocking the activity of such channels, neuromodulators can control the responsiveness of the cell to synaptic inputs

(Siegelbaum et al., 1982; Adams and Galvan, 1986; Brown, 1988; North, 1989; Yamada et al., 1989; Hille, 1992). These regulations can profoundly affect the function of neuronal circuits. For example, a change in firing properties during the transition from the sleep to the awake state produced by the neurotransmitter-mediated closing of a subthreshold-operating K$^+$ channel in thalamocortical neurons is thought to be responsible for the reestablishment of the faithful transmission of sensory information from the thalamus to the neocortex (Steriade et al., 1990, 1993; McCormick, 1992).

The application of molecular methods can be useful not only to identify the protein components of known K$^+$ channels, but it can also lead to the discovery of K$^+$ channel types that had not been previously identified through electrophysiological and pharmacological analysis (Pongs, 1992; Chandy and Gutman, 1995; Jan and Jan, 1997; Wang et al., 1998; Coetzee et al., 1999; Ganetzky et al., 1999; Rudy et al., 1999). Here we report the cloning of a cDNA encoding the principal components of a novel subthreshold-activating voltage-gated K$^+$ channel expressed by only a select population of CNS neurons. The protein (Eag2) is a member of the ether-à-go-go (Eag) family of K$^+$ channel pore-forming subunits (Drysdale et al., 1991; Warmke et al., 1991; Ludwig et al., 1994; Warmke and Ganetzky, 1994; Robertson et al., 1996) (for review, see Ganetzky et al., 1999). It is most similar to Eag1, the one presently known mammalian homolog of the *Drosophila* Eag gene, and has thus been named Eag2.

Some K$^+$ channel proteins are widely distributed in brain, whereas others have a more restricted pattern of expression and

may have functions that are specific to few neuronal systems (Chandy and Gutman, 1995; Jan and Jan, 1997; Coetzee et al., 1999; Rudy et al., 1999). Eag2 is a striking example of the latter group.

Members of the Eag family of K$^+$ channels display intriguing electrophysiological properties in heterologous expression systems and have been found to be the cause of human cardiac genetic disease (Curran et al., 1995; Sanguinetti, 1999), highlighting the importance of this channel family. However, little is known about their functions in native brain tissue. As in the case of Eag1, we find that when expressed in *Xenopus* oocytes, Eag2 expresses voltage-gated K$^+$ channels with unusual electrophysiological properties, including no measurable inactivation, and a strong dependence of activation kinetics on prepulse potential (Cole-Moore shift) (Ludwig et al., 1994; Robertson et al., 1996; Terlau et al., 1996). However, in contrast to Eag1, Eag2 activates at significantly more negative membrane potentials than Eag1. Thus, Eag2 channels could have strong influences on the subthreshold behavior of neurons containing these channels. The electrophysiological and histological studies presented here provide the basis for the identification of native Eag2 channels in brain neurons.

MATERIALS AND METHODS

Cloning of Eag2. RNA (1 μg) prepared from rat thalami (see below) was reverse-transcribed using Superscript reverse transcriptase (Life Technologies, Grand Island, NY) using random hexamers as primers. One microliter of this RT reaction was used as template in each of the following PCRs (with the exception of 5′ RACE reactions). All reactions (with the exception of 5′ RACE) were performed using PCR reagents from Perkin-Elmer following the manufacturers protocol with 2 mM MgCl and the following thermocycler protocol: 94° 1 min; 55° 1 min; 72° 1 min, 35 cycles. All PCR products (including 5′ RACE) were cloned directly into pCR2.1-TOPO vector (Invitrogen, Carlsbad, CA), with the exception of fragment F (see below), which was cloned into the pGEM-TEasy vector (Promega, Madison, WI), for sequencing and/or further manipulations.

An alignment of all known Eag1 protein sequences was used to design a pair of degenerate primers: forward CCCTACGACGTGAT(ACT)A-A(CT)GC(N)TT(CT)GA and reverse CCAGGTGCTCAC(N)A(CT) (GA)TA(AG)TCCAT. These primers were used in a PCR using rat thalamic cDNA as a template and yielded a single novel 636 bp partial Eag sequence (fragment A) that was 77% identical at the nucleotide level to the rat Eag1 (rEag1) cloned previously by Ludwig et al., (1994). No amplification of rEag1 was observed in this or any other PCR reaction that used thalamic cDNA as template. This was not surprising because Eag1 is not expressed in rat thalamus (Ludwig et al., 1994; M. Saganich and B. Rudy, unpublished observations).

At the same time, a screen of the human expressed sequence tag (EST) database for Eag homologs revealed a new (1700 bp) partial human Eag sequence (U69185), which was 60% identical at the amino acid level to rEag1. To obtain the rat homolog of this apparently new Eag protein, degenerate primers based on the human EST were developed: forward CGGAAGGTTTT(CT)(AG)A(N)GA(AG)CA(CT)C and reverse CT-GCTCGGG(TGA)AT(TGCA)GG(GA)TA(GA)AA. This PCR yielded a single 1089 bp product (fragment B) that was 96% identical to the human EST and 58% identical to rEag1 at the amino acid level. A PCR with specific primers derived from the 3′ end region of fragment A (forward TGTATGCCAACACCAACCG) and the 5′ end region of fragment B (reverse ACACTCTCTCCAGCATGGTA) produced a DNA fragment of 333 bp (fragment C), indicating that nonoverlapping fragments A and B were part of the same transcript and defined a novel partial Eag protein (Eag2), incomplete at the 5′ and 3′ ends.

The 3′ end of the clone was completed by another PCR using a forward primer derived from the sequence of fragment B (CGGAAGGTTTT-T(CT)(AG)A(N)GA(AG)CA(CT)C) and a reverse primer from the 3′ untranslated region (UTR) of the human EST: CAGAATCCAGCTG-GACATGC. This reaction yielded a single 1526 bp product (fragment D) and included a stop codon (TAA) in frame and 182 bp of 3′ UTR sequence.

Completion of the 5′ end of Eag2 was achieved by two rounds of 5′ rapid amplification of cDNA ends (5′ RACE) using an adaptor-ligated cDNA library from rat brain (Clontech, Palo Alto, CA) and Advantage cDNA polymerase (which has 3′→5′ proofreading activity) following the manufacturers protocols (Clontech). The initial RACE reaction used a gene-specific primer derived from the 3′ end of fragment C (GCGTCA-CACTCTCTCCAGCATGGTA) and adapter primer 1 (AP1) (supplied by the manufacturer). From this reaction we isolated fragment E, which included 1589 bp of novel sequence but did not reach the starting methionine. A nested RACE reaction was performed with gene specific primer AGGTAATGGTCCAGTTTCCTA, derived from the sequence of fragment G (see below), and nested adapter primer 2 (AP2) (supplied by the manufacturer) using reaction products from the first RACE diluted 1:50 in ddH$_2$O as template. This reaction resulted in a 1248 bp clone (fragment F) that included the putative starting methionine and 225 bp of 5′ UTR sequence. The thermocycling protocol was 94° 1 min; 5 cycles: 94° 30 sec, 72° 4 min; 5 cycles: 94° 30 sec, 70° 4 min; 25 cycles: 94° 20 sec, 68° 4 min for the first RACE reaction, and 94° 1 min; 55° 1 min; 72° 1 min, 35 cycles for the nested reaction. RACE products from both the initial and nested RACE reactions were identified by Southern blot (Sambrook et al., 1989) probed with a 930 bp N-terminal fragment of Eag2 (fragment G) obtained by PCR using forward degenerate primer AATGCCCA(AG)AT(ACT)GT(N)GA(CT)TGG, derived from the alignment of known Eag sequences, and specific primer AGGTAATG-GTCCAGTTTCCTA derived from the sequence of fragment A. RACE products, which hybridized with the Eag2 fragment G probe, were subsequently gel-purified using Qiaex II (Qiagen, Valancia, CA) following manufacturers instructions, ligated into the pCR2.1-TOPO vector, and transformed into chemically competent DH5α (Life Technologies) by a standard heat-shock method (Sambrook et al., 1989). Individual clones were identified by colony hybridization (Sambrook et al., 1989) using Eag2 fragment G probe.

The full-length clone was completed by the ligation of restriction fragments of the overlapping RACE products E and F with a restriction fragment of D in pCR2.1-TOPO vector using restriction sites *Aat*II and *Bsm*I. Briefly, recombinant plasmids containing fragment F were restricted with *Not*I, located in the multiple cloning site (MCS) of pGEM-TEasy and *Aat*II, and this fragment was gel-purified. Recombinant plasmids containing fragment E were restricted with *Aat*II and *Bsm*I and gel-purified. Fragment D was restricted using *Not*I (located in the MCS of pCR2.1-TOPO) and *Bsm*I and also gel-purified. All three purified fragments were ligated in a single reaction, and plasmids containing the full sequence in proper orientation were selected, resulting in a full-length clone in the pCR2.1-TOPO vector that was fully sequenced on both strands. For oocyte expression, the full-length Eag2 clone was subcloned into pSGEM vector (containing the 5′ and 3′ UTR of *Xenopus* βGlobin) (Liman et al., 1992) using *Bam*HI and *Eco*RI restriction sites. Two Eag2 isolates were used as templates for the synthesis of cRNA (see below), and both expressed the same currents in *Xenopus* oocytes.

Preparation of cDNA probes for Northern/Southern blot analysis and in situ *hybridization histochemistry.* Fragments G (bp 92–1022) and B (bp 1650–2708) from the NH$_2$ and C termini, respectively, were prepared by PCR and used to synthesize radiolabeled probes for Southern blot, *in situ* hybridization, and Northern blot analysis. Both fragments showed <80% nucleotide identity with other sequences in the Eag family. These two fragments gave identical results, and there was no cross-reactivity with Eag1 under the hybridization conditions used in our experiments because Eag2 and Eag1 probes labeled distinct structures in the brain and recognized bands of different sizes in *in situ* hybridizations and Northern blots [data not shown; also see Ludwig et al. (1994)].

Fragments G and B were released from the pCR2.1-TOPO vector with *Eco*RI, gel-purified, and phenol/chloroform-extracted followed by EtOH precipitation. Radioactive probes were obtained by labeling these fragments by the random hexamer primer method with ^{32}P-α-dCTP for Northern and Southern blot analysis, or with ^{35}S-α-dCTP for *in situ* hybridization histochemistry using the Roche Molecular Biochemicals Random Prime cDNA labeling kit following manufacturers instructions.

Preparation of poly(A) RNA. Total RNA from thalamus, olfactory bulb, and cerebral cortex were isolated from freshly dissected brains obtained from 20-d-old Sprague Dawley rats by the acid guanidinium-thiocyanate-phenol-chloroform procedure (Chomczynski and Sacchi, 1987). The RNA was poly(A)-selected by oligo-dT column chromatography (type 2 poly-T Sepharose, Collaborative Biomedical Products) following the protocol of Sambrook et al. (1989). The RNA was ethanol-precipitated

twice and resuspended in RNase-free water at a concentration of ~1 mg/ml and stored at −70°C.

RT-PCR analysis of Eag2 expression. The tissue distribution of Eag2 mRNAs was determined using RT-PCR from poly(A) RNA derived from several rat tissues (Clontech). Poly(A) RNA (1 μg) from each tissue was reverse-transcribed using Superscript reverse transcriptase (Life Technologies) using random hexamers as primers in a total volume of 25 μl. One microliter of each RT reaction was used as template for PCR. Eag2 specific primers were forward TGTATGCCAACACCAACCG and reverse ACACTCTCTCCAGCATGGTA. Glyceraldehyde 3-phosphate dehydrogenase (GAPDH) primers (forward ACCACAGTCCATGC-CATCAC; reverse TCCACCACCCTGTTGCTGTA) were used as controls to determine the integrity of the cDNA synthesized in the RT reaction. The PCR thermocycling protocol was 94° 45 sec.; 55° 45 sec.; 72° 45 sec., 25 cycles.

Northern blot analysis. Olfactory bulb, cerebral cortex, and testes mRNAs were subjected to electrophoresis in denaturing formaldehyde gels and transferred to Duralon-UV membranes (Stratagene, La Jolla, CA) as previously described (Rudy et al., 1988). The Northern blots were hybridized at 68°C with the ^{32}P-radiolabeled DNA probes under high stringency using Quickhyb solution (Stratagene), washed at 60°C in 0.1× SSC (Life Technologies) with 0.1% SDS, and exposed to x-ray film at −70°C for 14 hr.

In situ *hybridization histochemistry. In situ* hybridization was performed using the methods described in Stone et al. (1990) and Weiser et al. (1994). Briefly, 4- to 6-week-old male rats were perfused intracardially with 100 ml of cold saline solution (0.9% NaCl with 0.5% NaNO$_2$ and 1000 U heparin), followed by 300 ml of cold 4% paraformaldehyde solution in 0.1 M phosphate buffer, pH 7.4. The brains were carefully removed, cut in blocks, and post-fixed for 1 hr. After post-fixing, the brains were washed several times in cold, 0.1 M phosphate buffer, pH 7.4, and placed in 30% sucrose overnight. Slices were obtained on a freezing-microtome at 40 μm thickness and prehybridized at 48–50°C in a solution containing 50% formamide, 2× SSC, 10% dextran sulfate, 4× Denhardt's, 50 mM dithiothreitol, and 0.5 mg/ml sonicated, denatured salmon sperm DNA. After 2 hr of prehybridization, heat-denatured, 10^7 counts of ^{35}S-radiolabeled probe were added, and the hybridization reaction was allowed to proceed for 17 hr. After hybridization, the sections were washed in decreasing concentrations of SSC (2 to 0.1×) buffer at 48°C. After a final wash in 0.05 M phosphate buffer at room temperature, the sections were hand-mounted on gelatin-coated slides and air-dried. The slides were exposed to DuPont Microvision-C x-ray film for 7 d. The slides were then dipped in prewarmed Kodak NTB-2 photographic emulsion and exposed for 2 weeks at 4°C in the dark. The slides were developed in Kodak D-19 solution, fixed, and counterstained with a cresyl violet solution. Data analysis and photography were performed with a Zeiss Axiophot photomicroscope.

Preparation of in vitro *transcribed RNA and expression in* Xenopus *oocytes.* Recombinant pSGEM plasmids containing the full-length Eag2 cDNAs were linearized by digestion with *Nhe*I. Templates for *in vitro* transcription were prepared from these digests as described in Iverson and Rudy (1990) and transcribed with T7 RNA polymerase using the Stratagene mCAP transcription kit (Stratagene) following the supplier's protocols. The products of the transcription reaction (cRNAs) were diluted in RNase-free water and stored at −70°C. Expression of the RNAs was performed by injection of 50 nl of cRNA into defolliculated stage V and VI oocytes from *Xenopus laevis* (Iverson and Rudy, 1990). The injected oocytes were incubated for 3–4 d at 18°C in ND96 (96 mM NaCl, 2 mM KCl, 1.8 mM CaCl, 1 mM MgCl$_2$, 5 mM HEPES, buffer, pH 7.3–7.4) with 100 U/ml penicillin and 100 μg/ml streptomycin, filtered through a 0.45 μm membrane).

Electrophysiology. Currents were recorded under two-electrode voltage clamp with Geneclamp 500 amplifier (Axon Instruments, Foster City, CA) 1–7 d after RNA injection at room temperature (20–23°C). Electrodes were filled with 2 M KCl and had resistance of 0.5–1.0 MΩ. Currents were low-pass-filtered at 2 kHz. Data were acquired using pClamp 6.0 software (Axon Instruments). Data analysis and curve fitting were performed using Clampfit and/or Origen 4.0 software (Microcal, Amherst, MA). The recording chamber was continually perfused with ND96 unless otherwise noted. Osmolarity was maintained in high K, TEA, or 4-AP solutions by equimolar replacement of Na with the given cation.

RESULTS

Cloning and primary structure of rat Eag2

The Eag family of K$^+$ channel pore-forming subunits was identified after the cloning of the ether-à-go-go (Eag) gene in *Drosophila* (Drysdale et al., 1991; Warmke et al., 1991; Warmke and Ganetzky, 1994). The family includes three subfamilies known as Eag, Erg, and Elk (Ganetzky et al., 1999). There is presently one known member of the Eag subfamily in mammals (Eag1), but there are several Erg and Elk genes (Ludwig et al., 1994; Robertson et al., 1996; Shi et al., 1997, 1998; Engeland et al., 1998; Frings et al., 1998; Trudeau et al., 1995, 1999).

We identified Eag2 in a screen for K$^+$ channel transcripts expressed in the rat thalamocortical system. As part of this screen, a novel sequence was amplified from thalamic cDNA in a PCR that used degenerate PCR primers designed to amplify Eag proteins (see Materials and Methods). The sequence was 77% identical to rat Eag1 (Ludwig et al., 1994) at the amino acid level. RT-PCR and 5′ RACE were used to obtain a complete coding sequence (see Materials and Methods). This resulted in a 3374 bp cDNA with a single open reading frame of 2964 bp, predicting a protein of 988 amino acids and 112 kDa (Fig. 1).

Comparison of the amino acid sequence of Eag2 with the sequence of rat Eag1 and members of the Erg and Elk subfamilies shows that the new sequence is much more similar to Eag1 (and *Drosophila* or *Caenorhabditis elegans* Eag) than to Erg and Elk proteins (Table 1). The new sequence is therefore a member of the Eag subfamily and was named Eag2. Rat Eag2 is very similar to rat Eag1, with an overall amino acid sequence identity of 74% and a similarity of 82%.

Hydropathy analysis predicts that Eag2 has six membrane spanning domains (data not shown). The protein shares the overall structure of other proteins of the Eag family (Fig. 1). Like other K$^+$ channel proteins of the S4 superfamily, Eag proteins contain a core membrane region consisting of six putative membrane-spanning domains designated S1 to S6 flanked by amino and carboxyl domains of variable lengths that are thought to be intracellular (Pongs, 1992; Chandy and Gutman, 1995; Jan and Jan, 1997; Coetzee et al., 1999). Domains S1–S3 and S5–S6 are hydrophobic and thought to span the membrane as α helices. The S4 domain, a critical component of the voltage sensor, is amphipathic and characterized by the repetition of a motif consisting of a charged residue (R or K) and two hydrophobic or neutral amino acids. The motif is repeated five times in Eag2 as in other Eag proteins (Fig. 1) (Pongs, 1992; Sigworth, 1994; Caterall, 1995; Jan and Jan, 1997; Ganetzky, 1999).

Eag2 also contains the characteristic pore (P or H5) domain, present between the fifth and the sixth membrane spanning domains. This is highly conserved among distinct K$^+$ channel pore-forming subunits and is believed to contribute to the formation of the channel's K$^+$ selective pore (MacKinnon and Yellen, 1990; Hartmann et al., 1991; Yool and Schwarz, 1991; Pongs, 1992; Chandy and Gutman, 1995; Jan and Jan, 1997; Doyle et al., 1998). As in other members of the Eag family (as well as some members of the inward rectifying and two-pore family of K$^+$ channel subunits), the signature sequence GYG is replaced by GFG in Eag2 (Warmke and Ganetzky, 1994; Ganetzky et al., 1999). As in all other members of the Eag family (including Ergs and Elks), the Eag2 protein contains a sequence of unknown function (labeled as cNBD in Fig. 1) similar to the cyclic nucleotide binding domain found in cyclic nucleotide-gated and pace-
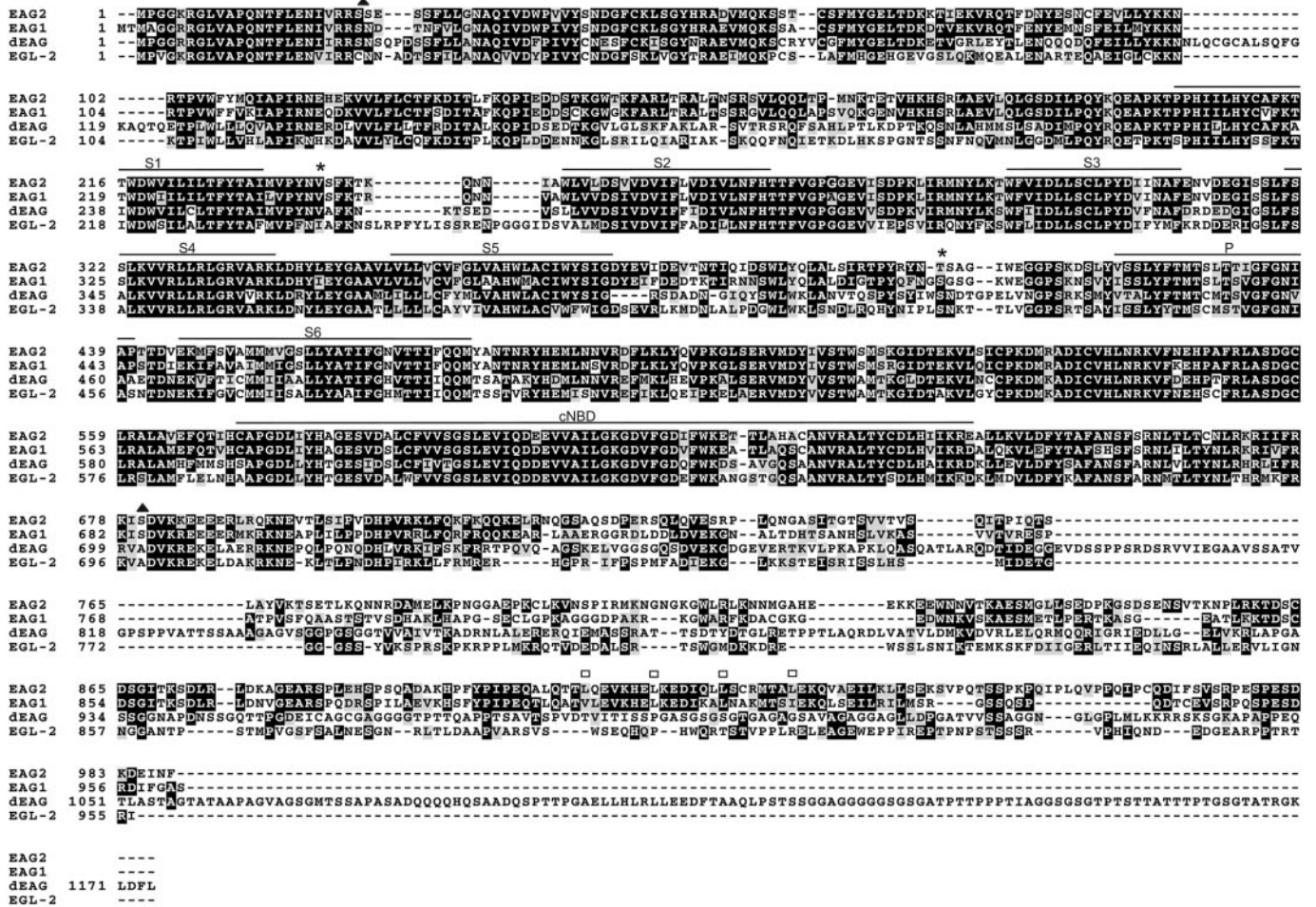
```
EAG2    1   --MPGGKRGLVAPQNTFLENIVRRSSE---SSFLLGNAQIVDWPVVYSNDGFCKLSGYHRADVMQKSST--CSFMYGELTDKKTIEKVRQTFDNYESNCFEVLLYKKN------------
EAG1    1   MTMAGGKRGLVAPQNTFLENIVRRSND---TNFVLGNAQIVDWPIVYSNDGFCKLSGYHRAEVMQKSSA--CSFMYGELTDKDTVEKVRQTFENYEMNSFEILMYKKN------------
dEAG    1   --MPGGKRGLVAPQNTFLENIIRRSNSQPDSSFLLANAQVVDVFPIVYCNESFCKLSGYNRAEVMQKSCRYVCGFMYGELTDKETVGRLEYTFLENQQQDQFEILLYKKNNLQCGCALSQFG
EGL-2   1   --MPVGKRGLVAPQNTFLENVIRRCNN-ADTSFTLANAQVVDYPIVYCNDGFSKLVGYTRAEIMQKPCS--LAFMHGEHGEVGSLQKMQEALENARTEQAEIGLCKKN------------

EAG2    102 -----RTPVWFYMQIAPIRNEHEKVVLFLCTFKDITLFKQPIEDDSTKGWTKFARLTRALTNSRSVLQQLTP-MNKTETVHKHSRLAEVLQLGSDILPQYKQEAPKTPPHIILHYCAFKT
EAG1    104 -----RTPVWFFVKIAPIRNEQDKVVLFLCTFSDITAFKQPIEDDSTKGWGKFARLTRALTSSRGVLQQLAPSVQKGENVHKHSRLAEVLQLGSDILPQYKQEAPKTPPHIILHYCVFKT
dEAG    119 KAQTQEPVWLLLQVAPIRNERDLVVLFLLTFRDITALKQPIDSEDTKGVLGLSKFAKLAR-SVTRSRQFSAHLPTLKDPTKQSNLAHMMSLSADIMPQYRQEAPKTPPHILHYCAFKA
EGL-2   104 -----KTPIWLLLVHLAPIKNHKDAVLYLGQFKDITPLKQPLDDENNKGLSRILQIARIAK-SKQQFNQIETKDLHKSPGNTSSNFNQVMNLGGDMLPQYRQETPKTSPHILHYSSFKT

                    S1                  *                              QNN----      IANLVLDSVVDVIPLVDIVLNPHTTFVGPGEVISDPKLIRMNYLKTWFVIDLLSCLPYDIINAFENVDEGISSLFS
EAG2    216 TWDWVILILTFYTAIMVPYNVSFKTK---------QNN----IANLVLDSVVDVIPLVDIVLNPHTTFVGPGEVISDPKLIRMNYLKTWFVIDLLSCLPYDIINAFENVDEGISSLFS
EAG1    219 TWDWIILILTFYTAILVPYNVSFKTR---------QNN----VAWLVVDSIVDVIPLVDIVLNFHTTFVGPNGEVISDPKLIRMNYLKTWFVIDLLSCLPYDIINAFENVDEGISSLFS
dEAG    238 IWDWVILCLTFYTAIMVPYNVAFKN---------KTSED-----VSLLVVDSIVDVIPFIDIVLNFHTTFVGPGGEVVSDPKVIRMNYLKSWFIIDLLSCLPYDVFNAFDRDEDGIGSLFS
EGL-2   218 IWDWSIILALTFYTAFMVPFNIAPKNSLRPFYLISSRENPGGGIDSVALMDSIVDVIPFADILLNFHTTFVGPGGEVVIEPSVIRQNYFKSWFLIDLLSCLPYDIFYMFKRDDERIGSLFS

                S4                        S5                                *   TSAG--    IWEGGPSKDSLYVSSLYFTMTSLTTIGFGNI
EAG2    322 SLKVVRLLRLGRVARKLDHYLEYGAAVLVLLVCVFGLVAHWLACIWYSIGDYEVIDEVTNTIQIDSWLYQLALSIRTPYRYN-TSAG--IWEGGPSKDSLYVSSLYFTMTSLTTIGFGNI
EAG1    325 SLKVVRLLRLGRVARKLDHYLEYGAAVLVLLVCVFGLAAHWLACIWYSIGDYEIFDEDTKTIRNNSWIYQLALDIGTPYQYNFNGSGSG--KWEGGPSKNSVYISSLYFTMTSLTSVGFGNI
dEAG    345 ALKVVRLLRLGRVIRKLDRYLEYGAAMLILLLCFYMLVAHWLACIWYSIG-----RSDADN-GIQYSWLWKLANVTQSPYSYIWSNDTGPELVNGPSRKSMYVTALYFTMTCMTSVGFGNV
EGL-2   338 ALKVVRLLRLGRVARKLDNYLEYGAATLLLLLCAYVIVAHWLACVWFWIGDSEVRKLDKMDNLALPDGWLWKLSNDLRQHYNIPLSNKT--TLVGGPSRTSAYISSLYVTMSCMSTVGFGNI

                                        S6                                                              cNBD
EAG2    439 APTTDVEKMFSVAMMMVGSLLYATIFGNVTTIFQQMYANTNRYHEMLNNVRDFLKLYQVPKGLSERVMDYIVSTWSMSKGIDTEKVLSICPKDMRADICVHLNRKVFNEHPAFRLASDGC
EAG1    443 APSTDLEKIFAVAIMMIGSLLYATIFGNVTTIFQQMYANTNRYHEMLNNVRDFLKLYQVPKGLSERVMDYIVSTWSMSKGIDTEKVLQICPKDMRADICVHLNRKVFKEHPAFRLASDGC
dEAG    460 AAETDNEKVTICMMIIAALLYATIFGNVTTIIQQMYSATAKYHDMLNNVREPMKLHEVPKALSERVMDYIVSTWANTKGLDTEKVLNCCPKDMRADICVHLNRKVFDEHPTFRLASDGC
EGL-2   456 ASNTDNEKIFGVCMMIISALLYAAIFGHMTTIIQQMYSSTVRYHEMISNVREPIKLQEIPKELAERVMDYVVSTWANTKGIDTAKVLGYCPKDMRADICVHLNRKVFNEHSCFRLASDGC

EAG2    559 LRALAVEFQTLHCAPGDLIYHAGESVDALCFVVSGSLEVIQDVAILGKGDVFGDIFWKET-TLAHACANVRALTYCDLHIKKREALLKVLDFYTAFANSFSRNLTLTCNLRKRIIFR
EAG1    563 LRALAMEFQTVHCAPGDLIYHAGESVDSLCFVVSGSLEVIQDDEVVAILGKGDVFGDVFWKEA-TLAQSCANVRALTYCDLHVIKRDALQKVLEFYTAFSHSFSRNLILTYNLRKRIVFR
dEAG    580 LRALAMHFMMSHSAPGDLYHAGESIDSLCFIVTGSLEVIQDDEVVAILGKGDVFGDVFWKDS-AVGQSAANVRALTYCDLHAIKRDLLLEVLDFYSAFANSFARNLVLTYNLRHRLIFR
EGL-2   576 LRSLAMFLELNHAAPGDLLYHTGESVDALWFVVSGSLEVIQDDEVVAILGKGDVFGDEFWKANGSTGQSAANVRALTYSDLHMIKKDRLMDVLDFYKAFANSFARNTMLTLTYNLTHRMKFR

                        ▲
EAG2    678 KISDVKREEEERLRQKNEVTLSIPVDHPVRKLFQKFKQQKELRNQGSAQSDPERSQLQVESRP--LQNGASTTGTSVVTVS------QITPIQTS-------------------------
EAG1    682 KISDVKREEEERMKRKNEAPLILPPDHPVRRLFQRFRQQKEAR-LAAERGGRDLDDLDVEKGN--ALTDHTSANHSLVKAS------VVTVRESP-------------------------
dEAG    699 RVADVKREKELAERRKNEPQLFQNQDHLVRKIFSKFRRTPQVQ-AGSKELVGGSGQSDKVREKGDGEVERTKVLPKAPKLQASQATLARQDTIDECEGEVDSSPPSRDSRVVIEGAAVSSATV
EGL-2   696 KVADVKREKELDAKRKNE-KLTLPNDHPIRKLLFRMRER-----HGPR-IFPSPMFADIEKG---LKKSTEISRISSLHS-------MIDETG--------------------------

EAG2    765 --------------LAYVKTSETLKQNNRDAMELKPNGGAEPKCLKVNSPIRMKNGNGKGWMRLKNNMGAHE---------EKKEEWNNVTKAESMGLLSEDPKGSDSENSVTKNPLRKTDSC
EAG1    768 --------------ATPVSFQAASTSTVSDHAKLHAPG-SECLGPRAGGGDPAKR----KGWARFKDACGKG---------EDWNKVSKAESMETPPERTKASG------BATLKKTDSC
dEAG    818 GPSPPVATTSSAAAGAGVSGGPGSGGTVVVIVTKADRNLALEREBQIEMASSRAT---TSDTYDTGLRETPPTLAQRDLVATVLDMKVDVRLELQRMQQRIGRIEDLLG--GLVKPLAPGA
EGL-2   772 --------------GG-GSS-YVKSPRSRPKRPPLMKRQTVDEDALSR----TSWGMDKKDRE---------WSSLSNIKTEMKSKFDIGERLTIIEQINSRLALLERVLIGN

                                            □      □      □      □      □
EAG2    865 DSGITKSDLR--LDKAGEARSPLEHSPSQADAKHPFYPIPEQALQTTLQEVKHELKEDIQLLSCRMTALEKQVAEILKLLSEKSVPQTSSPKPQIPLQVPPQIPCQDIFSVSRPESPESD
EAG1    854 DSGITKSDLR--LDNVGEARSPQDRSPILAEVKESFYPIPEQTLQATVLEVKHELKEDIKALNAKMTSIEKQLSEILRIIMSR-----GSSQSP-------------------------
dEAG    934 SSGGNAPDNSSGQTTPFGDEICAGCGAGGGGTPTTQAPFTSAVTSPVDTVITISSPGASGSGSGTGAGAGSAVAGAGGAGGLDPGATVVSSAGGN---GLGPLMLKKRRSKSGKAPAPPEQ
EGL-2   857 NGGCANTP-----STMPVGSFSALNESGN--RLTLDAAPVARSVS----WSEQHQP--HWQRTSTVPPLREELEAGEWEPPIREPTPNPSTSSSR------VPHIQND---EDGEARPPTRT

EAG2    983 KDEINF----------------------------------------------------------------------------------------
EAG1    956 RDIFGAS---------------------------------------------------------------------------------------
dEAG   1051 TLASTAGTATAAPAGVAGSGMTSSAPASADQQQQHQSAADQSPTTPGAELLHLRLLEEDFTAAQLPSTSSGGAGGGGGSGSGATPTTPPPTIAGGSGSGTPTSTTATTTPTGSGTATRGK
EGL-2   955 RI--------------------------------------------------------------------------------------------

EAG2        ----
EAG1        ----
dEAG   1171 LDFL
EGL-2       ----
```

Figure 1. Primary structure of Eag2. The amino acid sequence of Eag2 is compared with the sequence of rat Eag1 (Ludwig et al., 1994), *Drosophila* Eag (*dEAG*) (Warmke et al., 1991), and Eag from *C. elegans* (*EGL-2*) (g4731355). Gaps required to optimize the alignment are shown as *dashes*. Identical residues are shadowed *black*; similarities are shadowed in *gray*. The S1–S6 and P (or H5) domains as well as the cyclic nucleotide binding domain (*cNBD*) are *overlined*. *Triangles* indicate putative PKA-PKG phosphorylation sites in Eag2. *Asterisks* indicate putative N-glycosylation sites in Eag2. The leucines in the unique leucine heptad repeat in the C-terminal area of Eag2 are indicated with an *open square*. Putative PKC phosphorylation consensus sequences in Eag2 are located at amino acids 73–75, 127–129, 142–144, 237–239, 142–144, 237–239, 322–324, 395–397, 478–480, 502–504, 521–523, 773–775, 925–927, 943–945, 952–9254, 981–983.

maker channel families (Broillet and Firestein, 1999; Santoro and Tibbs, 1999).

The putative intracellular amino terminal sequence, the membrane-spanning, and cyclic nucleotide domains of Eag2 and

Table 1. Amino acid identity among the Eag family of potassium channel proteins

	Eag1 (%)	Erg1 (%)	Erg2 (%)	Erg3 (%)	Elk1d (%)	Elk1p (%)	Elk2 (%)
Eag2	74	31	31	30	30	29	29
Eag1		32	32	33	30	30	30
Erg1			64	57	31	35	32
Erg2				61	34	36	34
Erg3					31	31	29
Elk1d						54	46
Elk1p							48

The full-length Eag, Erg, and Elk amino acid sequences from rat were aligned using Clustal W (Thomson et al., 1994). Sequences used in the alignment were rEag2, reported in this paper; rEag1 (Ludwig et al., 1994); rErg1 (Bauer et al., 1998); rErg2 and rErg3 (Shi et al., 1997); rElk1d (Shi et al., 1998); rElk1p and rElk2 (Engeland et al., 1998).

other Eag proteins are very well conserved. Divergence from the Eag1 protein sequence is concentrated to the C-terminal region following the putative cyclic nucleotide binding domain (residues 720–842). Interestingly, this area has been implicated in Eag1 as the association site for interaction with an associated (β) subunit KCR1 (Hoshi et al., 1998). A leucine-zipper motif (residues 913–960) is present in Eag2 and contains four leucines repeated every seven residues. The same area in Eag1 is only 42% identical and contains only two leucines in heptat repeat (Fig. 1). Mutational analysis of this area in Eag1 has recently implicated it as a site for multimerization and subunit interactions (Ludwig et al., 1997). Sequence divergence found within these two regions may have interesting functional consequences for Eag2 and/or its association with other family members and/or accessory subunits.

Unlike in the Kv family, the primary sequence of all members of the Eag family, now including Eag2, shares a region of high similarity at the N terminus of the protein. Recently this domain (residues 1–134), referred to as the "Eag domain," was crystallized from human Erg (HERG) (Morais Cabral et al., 1998). The crystal structure revealed the Eag domain as a member of the
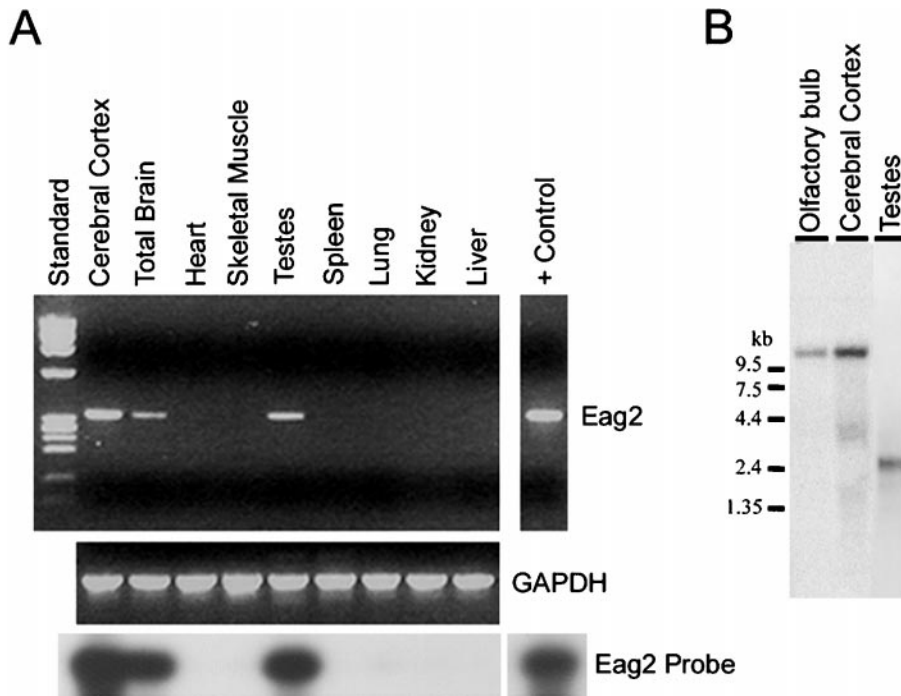
Figure 2. Tissue expression of Eag2. *A*, RT-PCR of rat mRNA prepared from various tissues using Eag2-specific primers (*top*) or GAPDH primers (*middle*). + *Control* (positive control) PCR from Eag2 cDNA. The reaction was analyzed on a 2% agarose gel stained with EtBr. A single PCR product was detected in the *Cerebral Cortex*, *Total Brain*, and *Testes lanes* only. A Southern blot using an Eag2 -specific probe (fragment B) confirmed the amplification of Eag2 in cerebral cortex, total brain, and testes (*bottom*). *B*, Northern blot of rat poly(A) RNA obtained from the olfactory bulb, cerebral cortex, or testes (2 μg per lane) hybridized with Eag2 fragment B probe.

PAS domain family. These domains have been previously found in proteins involved in the circadian rhythm as well as in prokaryotic proteins that have light and redox sensors (Ponting and Aravind, 1997; Zhulin et al., 1997; Morais Cabral et al., 1998; Reppert, 1998; Sassone-Corsi, 1998). PAS domains are thought to be involved in ligand as well as in protein–protein interactions (Hahn et al., 1997). The structural data of the PAS domain in human Erg, combined with mutational analysis of this domain in Erg and Eag1, have provided strong evidence that this N-terminal domain interacts with the body of the channel, perhaps with residues in the S4–S5 linker, affecting many aspects of channel gating, inactivation, and voltage sensitivity (Terlau et al., 1997; Morais Cabral et al., 1998; Chen et al., 1999)

Primary sequence analysis reveals that Eag2 shares with Eag1 a putative cAMP–cGMP-dependent protein kinase (PKA-PKG) phosphorylation site at amino acid position 677–680. It also contains a second, unique PKA-PKG site in the N terminus (residues 21–24) (Fig. 1). Eag1 also has multiple putative PKC sites. Eag2 shares many of these but also has three additional putative PKC phosphorylation sites located in the extreme C terminus that are not present in Eag1 (Fig. 1, see legend).

Eag2 is expressed at low levels in brain and testes but not in other tissues

RT-PCR was used to investigate the tissue distribution of Eag2 mRNA transcripts. (Fig. 2*A*). Strong signals were obtained from poly(A) RNA prepared from the cerebral cortex, brain, and testes. No signal was detected in heart, skeletal muscle, spleen, kidney, lung, or liver. A second RT-PCR of the testes cDNA, using another pair of Eag2-specific primers, confirmed the presence of Eag2 mRNA in this tissue (data not shown).

In situ hybridization of brain tissue suggests that Eag2 expression in brain is highly localized (see below). Consistent with the results from *in situ* hybridization, hybridization of a Northern blot prepared from mRNA derived from brain areas enriched in Eag2 transcripts (neocortex and olfactory bulb) identified a strong single ~12 kb transcript with higher levels found in cortex than in olfactory bulb. Signals from total brain were very weak (data not

Table 2. Comparison of electrophysiological properties of rat Eag2 and Eag1

	V_{on}	$V_{1/2}$ (mV)	Slope (mV^{-1})	τ activation (msec)[a]	Inactivation
Eag2	−100 mV[b]	−35.5[b]	29[b]	τ_{fast} = 14.6[b]	No inactivation during 7 sec depolarization[b]
				τ_{slow} = 202[b]	No inactivation at −30 mV for 5 min[b]
Eag1	−40 to −50 mV[c,d,f,h]	−11.8 to −4.1 mV[d,e,g]	23.5[d]	τ_{fast} = 12[f]	None reported[c–h]
				τ_{slow} = 210[f]	

[a]V = 40 mV.

[b]Reported in this paper.

[c]Ludwig et al., 1994.

[d]Robertson et al., 1996.

[e]Bijlenga et al., 1998.

[f]Frings et al., 1998.

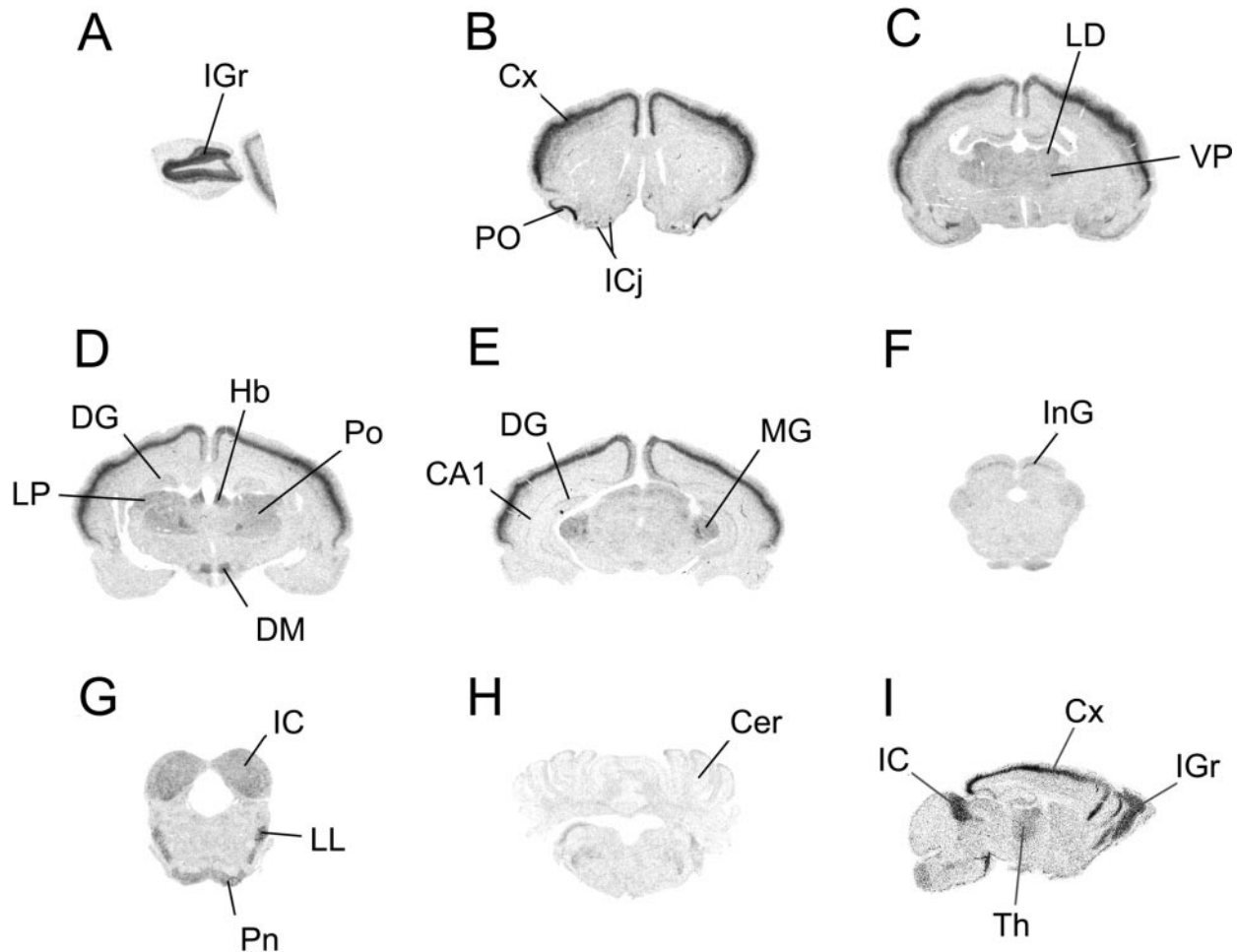[g]Schönherr et al., 1999.

[h]Terlau et al., 1996.

Figure 3. Distribution of Eag2 mRNAs in the rat and mouse brain. *A–H*, X-ray autoradiograms of coronal sections taken at different levels of rat brain after hybridization with the Eag2-specific ^{35}S-labeled probe (fragment B). *I*, X-ray autoradiogram of a sagittal section of a mouse brain after hybridization with the same probe as in *A–H*. Note the strong and laminar hybridization signals in the cerebral cortex (*Cx*). Other brain areas exhibiting strong signals include the granule cell layer of the olfactory bulb (*IGr*) and the olfactory cortex (*PO*). Moderate signals are seen in the Islands of Calleja (*ICj*), dorsal thalamic nuclei [as in the ventral posterior complex (*VP*), the laterodorsal nucleus (*LD*), the lateroposterior (*LP*), and posterior thalamic nuclear group (*Po*), as well as in the lateral geniculate nucleus (data not shown) and the medial geniculate (*MG*)], the habenula (*Hb*), the dorsomedial hypothalamic nuclei (*DM*), the intermediate gray layer of the superior colliculus (*InG*), the inferior colliculus (*IC*), the pontine nucleus (*Pn*), and the lateral lemniscus nuclei (*LL*). Weak to no signals are seen in the cerebellum (*Cer*) and hippocampus (CA1 area of the hippocampus, *CA1*; dentate gyrus, *DG*). *Th*, Thalamus.

shown). A Northern blot prepared from testes poly(A) RNA, however, identified a much smaller ~3 kb transcript, suggesting the possibility of an alternatively processed Eag2 transcript (Fig. 2*B*).

Eag2 is selectively expressed in a few neuronal populations in the brain and shows a unique laminar expression pattern in the cerebral cortex

The original RT-PCR that lead to the identification of Eag2 used mRNA derived from rat thalamus, indicating expression of Eag2 transcripts in this brain area. *In situ* hybridization histochemistry, using a probe from the C terminus (fragment B), was used to analyze the pattern of expression of Eag2 in adult rat and mouse brain. These experiments revealed that Eag2 is expressed in a few selected brain areas (Fig. 3). Strong signals were seen in the cerebral cortex, olfactory bulb, and primary olfactory cortex. Moderate to weak expression was seen in many dorsal thalamic nuclei, medial hypothalamic structures, superior and inferior colliculus, lateral lemniscus, pontine nuclei, and the Islands of Calleja. Overall, Eag2 expression was significantly different from

that of Eag1, which outside the CNS is also found in skeletal muscle (Ludwig et al., 1994; Bijlenga et al., 1998). Within the CNS, Eag1 expression is much more widespread, located most abundantly in cerebellum and hippocampus and at lower levels in the caudate/putamen, hypothalamus, and cerebral cortex (Ludwig et al., 1994; Saganich and Rudy, unpublished observations). Contrary to Eag1, no significant Eag2 expression was observed in the hippocampus, cerebellum, or caudate/putamen.

Most intriguing was the pattern of expression of Eag2 in the cerebral cortex, which is unlike that of Eag1 (Pongs, 1992; Chandy and Gutman, 1995; Coetzee et al., 1999). On x-ray film autoradiograms, the signal appeared as a dense narrow band located mainly toward the middle layers of the cortex (Fig. 3). This band was present throughout the anterior to posterior extent of the cerebral cortex, with the highest levels located within somatosensory cortex. In general, the signal became weaker and narrower as sections moved away from the somatosensory cortex in both the anterior and posterior direction. The band of Eag2 expression was also found throughout the entire dorsoventral extent of the
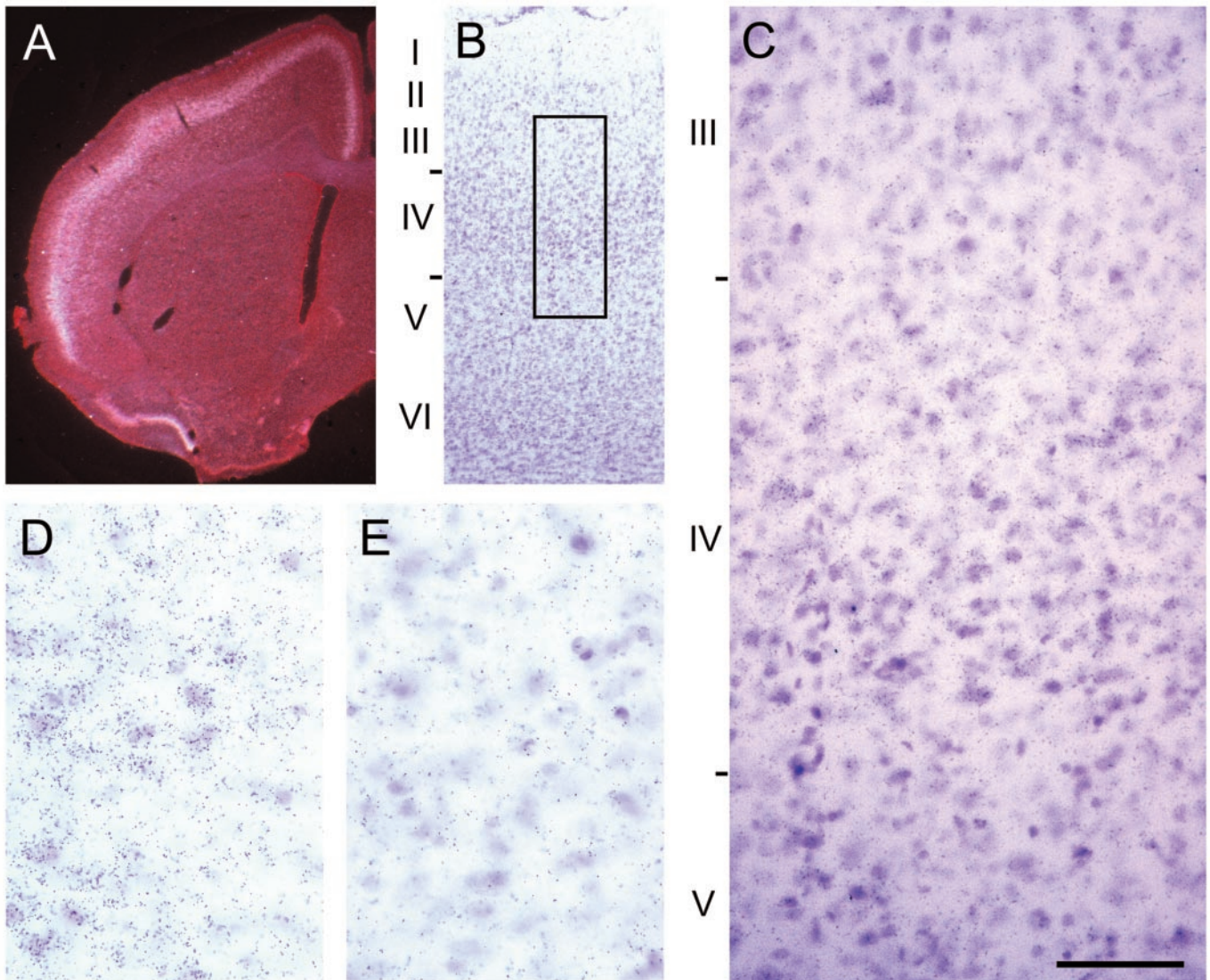
Figure 4. Expression of Eag2 in layer IV of the cerebral cortex. *A,* Dark-field image of a Nissl-stained coronal section through the rat neocortex hybridized with ^{35}S-labeled Eag2 probe (fragment B) and dipped in photographic emulsion. Note the laminar hybridization signal toward the middle of the cortex. The hybridization band is thicker in frontoparietal (somatosensory) cortex. Strong hybridization is also seen in the olfactory cortex and the islands of Calleja. *B,* Bright-field image of a portion of the section shown in *A,* illustrating the different cortical layers. Silver grains are difficult to distinguish at this amplification. *C,* Amplification of layer IV (*boxed section* in *B*). Note the increased concentration of silver grains over cells in layer IV. *D, E,* High magnification of cortical layers IV (*D*) and II-III (*E*). Note the large accumulation of silver grains over most cells in layer IV. In layer II-III the number of grains over cells is similar to background. Scale bar: *A,* 0.225 cm; *B,* 0.372 mm; *C,* 75 μm; *D, E,* 50 μm.

cerebral cortex, being broadest in somatosensory cortex (see cover). The expression pattern of Eag2 was confirmed in three separate experiments with the C-terminal probe. A different, nonoverlapping probe from the NH$_2$-terminus (fragment G) also gave identical results (data not shown). Preliminary data suggest that expression of Eag2 in brain appears to be conserved in both rat and mouse (Fig. 3*I*).

To further characterize the pattern of expression of Eag2 in the cerebral cortex, the S^{35}-hybridized sections were dipped in photographic emulsion, developed, and counterstained with a Nissl stain. Dark-field images confirmed our observations with x-ray autoradiograms. Signals were concentrated toward the middle lamina of the cortex, with little signal in deeper or more superficial layers (Fig. 4*A*). Bright-field microscopy of the Nissl-counterstained sections revealed that the greatest accumulation of silver grains was seen over layer IV (Fig. 4*B–D*). Observations

at high magnification showed that most neurons in layer IV had accumulated a large number of silver grains averaging 47.2 $\pm$ 2.7 grains per cell (Fig. 4*D*) in contrast to layers II-III, which had an average of 8.7 $\pm$ 1.9 grains per cell [a value similar to background (Fig. 4*E*)]. The number of heavily labeled cells decreases dramatically as one moves away from layer IV. This laminar-specific expression of Eag2 in the cerebral cortex is unlike that of any other potassium channel described to date and suggests that this protein may be particularly important for the function of neurons concentrated in layer IV (see Discussion).

Eag2 expresses subthreshold-activating, non-inactivating, voltage-dependent potassium currents in *Xenopus* oocytes

Most K$^+$ channel pore-forming subunits of the S4 superfamily produce tetrameric K$^+$ channels with specific characteristics
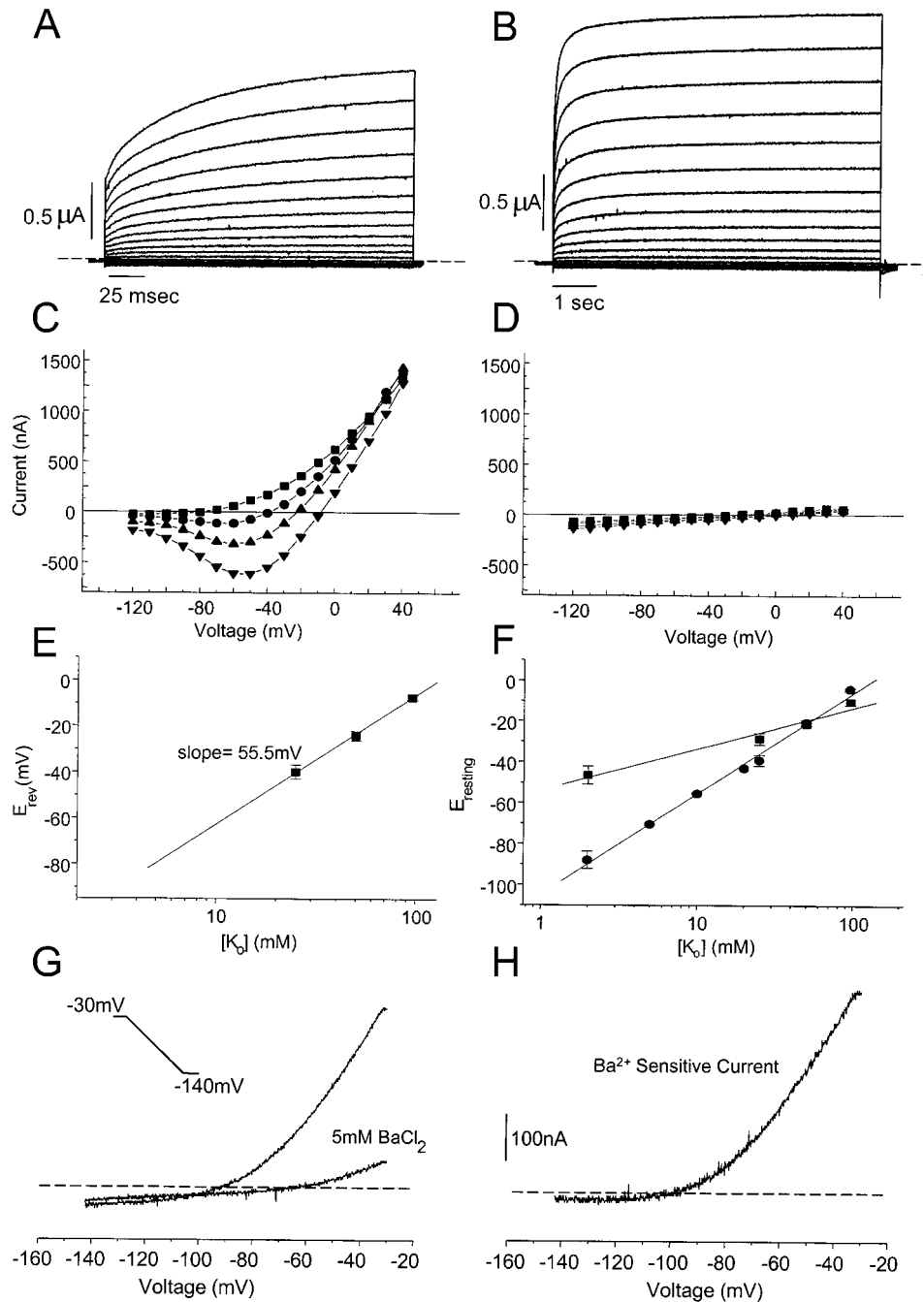
Figure 5. Eag2 expresses non-inactivating, subthreshold-activating K$^+$ currents in *Xenopus* oocytes. Expression of Eag2 currents by two-electrode voltage clamp. *A, B,* An oocyte injected with Eag2 cRNA was held at −90 mV, and a family of currents was measured using test potentials ranging from −120 to +40 mV. The duration of the test potentials was 214 msec in *A* and 7.4 sec in *B*. Bath contained ND96 in both experiments. *C–E,* Current–voltage relationship and K$^+$ permeability of Eag2 currents. Current–voltage (*I–V*) relationships of representative currents in an Eag2 cRNA-injected oocyte (*C*) or an uninjected oocyte (*D*) recorded in 2 mM (*squares*), 25 mM (*circles*), 50 mM (*triangles*), and 96 mM (*inverted triangles*) extracellular K$^+$. The currents were measured by two-electrode voltage clamp, with a holding potential of −90 mV and a voltage command series from −120 to +40 mV in 10 mV increments. *E,* Average reversal potentials ± SEM (*n* = 4) of Eag2 currents, determined from experiments such as in *C*, plotted as a function of the log of the [K$_o$]. A linear fit produced a line with a slope factor of 55.5 mV/decade. *F,* The resting potential of the oocytes was determined under current-clamp mode in different concentrations of extracellular K$^+$, and the average ± SEM resting potentials (*n* = 5) of Eag2-injected (*circles*) and uninjected (*squares*) oocytes was plotted as a function of log [K$_o$] and fit to straight lines. The slope factor for Eag2-injected and uninjected oocytes was 49.2 and 20.3 mV/decade, respectively. *G, H,* Eag2 currents evoked by slow voltage ramps. *G,* An Eag2-injected oocyte was held at −30 mV and then clamped to a slow (1.6 sec) hyperpolarizing ramp to −140 mV (see *inset*) in ND96 alone or in the presence of 5 mM BaCl$_2$. *H,* Ba^{2+}-sensitive current in *G* obtained by digital subtraction of the current after Ba^{2+} from the control current.

when expressed in *Xenopus* oocytes and other heterologous expression systems (Pongs, 1992; Chandy and Gutman, 1995; Jan and Jan, 1997; Coetzee et al., 1999). Injection of Eag2 cRNA in *Xenopus* oocytes resulted in large voltage-dependent outward currents, which were absent in uninjected or water-injected oocytes. The currents activated with membrane depolarization and exhibited no significant inactivation. The activation kinetics was complex, displaying both fast and slow components, and there was little sigmoidicity. Long (several seconds) depolarizations were required for the currents to approach steady-state values (Fig. 5*A,B*). Eag2 currents resembled most closely the currents expressed by Eag1 (Ludwig et al., 1994; Robertson et al., 1996; Terlau et al., 1996; Bijlenga et al., 1998; Frings et al., 1998), in accordance with their molecular relatedness.

Most interesting was the observation that outward currents were visible at very negative voltages (Fig. 5*A,B*). In fact, many Eag2-injected oocytes had small but sustained outward currents when holding at −90 mV, whereas uninjected oocytes have only sustained inward leak currents at this holding potential. To help visualize the currents at these hyperpolarized potentials, we increased the extracellular potassium concentration in the bath (standard external K$^+$ in ND96 is 2 mM). Under these conditions we were able to generate measurable inward currents at potentials more negative than the equilibrium potential for K$^+$ and were able to test the activity of the channel at very negative membrane potentials. Current–voltage relationships for the steady-state currents obtained in various extracellular K$^+$ concentrations show that currents, larger than those expected from leak, are already
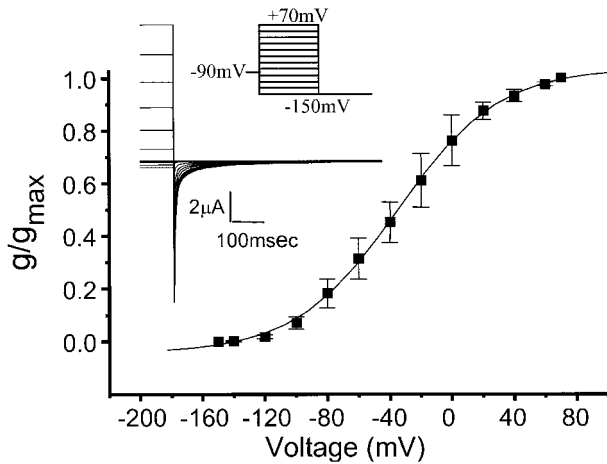
Figure 6. Normalized conductance–voltage relation for Eag2 channels. Instantaneous conductance $[G = I/(V - V_K)]$ as a function of voltage was obtained from measurements of instantaneous current that were obtained by extrapolating to time 0 the tail currents obtained at -150 mV after 2025 msec test pulses from -150 to $+70$ mV (see *inset*) in cells bathed in ND96 containing 25 mM KCl ($V_{holding} = -90$ mV). The values of conductance at a given voltage were normalized to the maximum conductance, and the average values $\pm$ SEM from four different oocytes were plotted as a function of voltage. The smooth curve is the fit to a Boltzmann function with a midpoint of -35.5 mV and a slope factor of 29 mV.
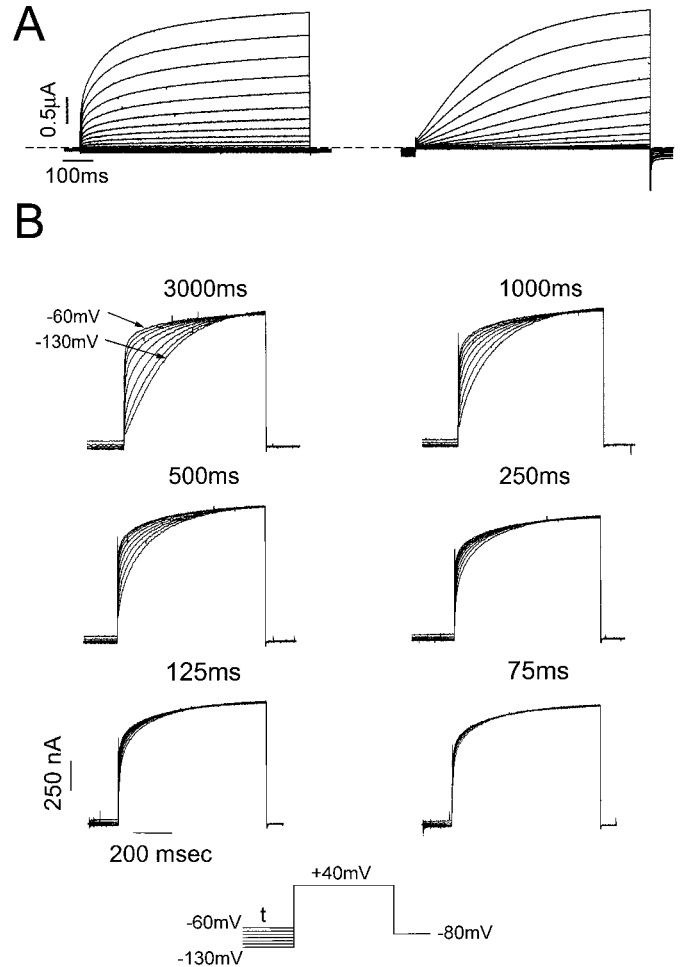

Figure 7. Effect of holding potential and prepulse duration on Eag2 currents in *Xenopus* oocytes. *A*, Currents in an Eag2-injected oocyte during test depolarizations of 800 msec ranging from -90 to $+40$ in 10 mV increments from a holding potential of -90 mV *(left)* or -120 mV *(right)*. Bath contained ND96 solution in both experiments. *B*, Evoked Eag2 currents during 800 msec test depolarizations to $+40$ mV, preceded by prepulses ranging from -130 to -60 mV with various duration (*t*) (as indicated above each panel) from 75 to 3000 msec. Holding potential was -80 mV, and bath solution contained ND96.

detectable at potentials between -100 and -90 mV (Fig. *5C*). Such currents were never seen in uninjected oocytes (Fig. *5D*). In all cases the current reversed at values near the reversal potential for potassium (E_K). Reversal potentials determined from the change of tail current direction in various extracellular K+ concentrations were also close to E_K (data not shown). A plot of the reversal potential obtained from I–V plots as a function of the log of extracellular potassium concentration resulted in a line with a slope of 55.5 mV, close to the theoretical value of 58 mV, indicating that the channels are highly selective for potassium (Fig. *5E*).

Because the current activated at such negative voltages, it was observed that oocytes expressing significant levels of Eag2 had resting potentials that were very close to E_K through a range of different extracellular potassium concentrations down to 2 mM. In contrast, the resting potentials of uninjected oocytes were much less sensitive to changes in extracellular potassium (Fig. *5F*).

Because the currents do not inactivate, it was possible to obtain current–voltage relationships for Eag2 currents using slow (1.6 sec) voltage ramps. As described below, Eag2 currents are blocked by extracellular Ba^{2+} (Fig. *5G*; see Table 3). We used this blocker to isolate the current mediated by Eag2 during depolarizing ramps (Fig. *5H*). These experiments confirmed that Eag2 currents activated at around -100 mV even in low (2 mM) K_o.

To determine the Eag2 conductance–voltage relationship, we measured instantaneous conductances from tail currents evoked at -150 mV after a series of voltage prepulses between -150 and 70 mV in 25 mM $[K]_o$ (Fig. *6, inset*). The values of instantaneous conductance $[g = I/(V - V_K)]$ were obtained from the instantaneous currents measured by fitting a double exponential function to the tail current (I) traces and extrapolating to $t = 0$, and using a reversal potential of -37 mV. The instantaneous conductance versus voltage plot was fitted to a Boltzmann function ($G/G_{max} = 1/\{1 + [\exp(V_m - V_{1/2})k]\}$). From these fits, we derived a midpoint of activation of -35.5 mV and a steepness parameter of 29 mV (Fig. *6*).

The midpoint of activation of Eag2 currents was considerably more negative to the previously published values for mouse and human Eag1, which range from -11 to -4.1 mV (Robertson et al., 1996; Bijlenga et al., 1998; Schönherr et al., 1999). The considerable differences in voltage dependence are the most important difference we have observed so far between Eag1 and Eag2 currents (Table 2).

Activation kinetics

Unlike most voltage-gated K+ channels of the Kv family, but similar to Eag1, the kinetics of activation of Eag2 is strongly influenced by the membrane potential before the test depolarization. For example, when the holding potential was changed from -90 to -120 mV, the activation kinetics of evoked currents became much slower and more sigmoidal in shape (Fig. *7A*). To further characterize the effect of prepulse voltage on channel activation, we provided a series of 1 sec conditioning prepulses to different voltages before a single test pulse to $+40$ mV (Fig. *8A*). The observed decrease in the speed of activation as the prepulse voltage is moved in the hyperpolarized direction was similar to
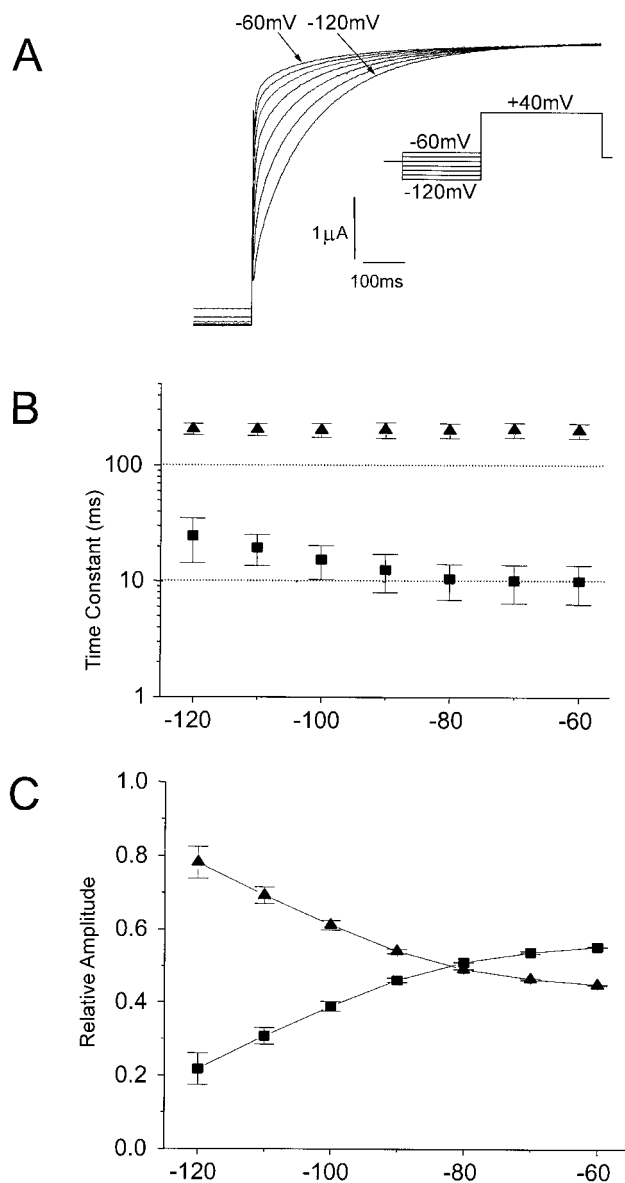
Figure 8. Hyperpolarizing prepulses slow down the activation of Eag2 currents. *A*, Currents in an Eag2 cRNA-injected oocyte during 800 msec test depolarizations to +40 mV, preceded by 1 sec prepulses ranging from −120 to −60 mV (holding potential −80 mV; bath solution ND96). The time course of the currents in experiments such as the one shown in *A* was approximated by the sum of two exponentials and the average ± SEM (*n* = 4) time constants and relative amplitudes of the exponentials plotted as a function of prepulse potential in *B* and *C*, respectively.

that seen with Eag1 (Ludwig et al., 1994; Robertson et al., 1996; Terlau et al., 1996) and resembles, but is not identical to, the nonsuperimposable Cole-Moore shift observed in potassium currents in crayfish axons (Young and Moore, 1981). To quantify this effect, the rise times of the currents were approximated by double exponential functions in several oocytes, and the average time constants and amplitudes were plotted as a function of prepulse potential (Fig. 8*B*,*C*). It was concluded that the main effect of prepulse voltage was to change the relative contributions of the fast and slow components. The time constant of the fast component also became slightly faster as the prepulse potential increased, ranging from 25 to 10 msec. The time constant of the
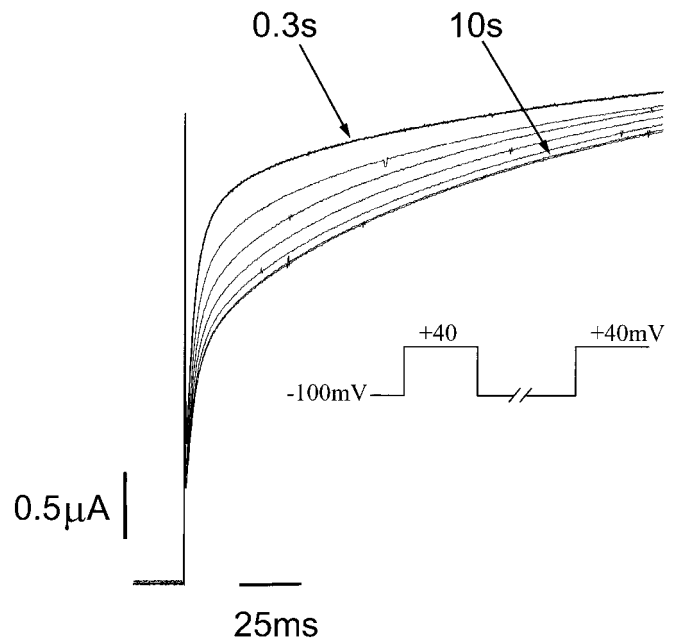
Figure 9. Slow recovery of the changes in activation kinetics of Eag2 currents produced by a previous depolarization. Superimposed currents evoked by the second test potential of a two-pulse protocol with increasing interpulse intervals. The voltage protocol (see *inset*) included two square pulses of 210 msec duration to +40 mV separated by interpulse periods at −100 mV of 0.3, 0.5, 1, 2, 4, 8, and 10 sec. Holding potential: −100 mV.

slow component, however, remained relatively constant at 202 ± 2 msec regardless of the prepulse potential.

These effects of prepulse potential indicate that the kinetics of Eag2 channel opening in a particular cell could vary depending on previous changes in the cell membrane potential. To obtain an idea of whether physiological conditions could influence channel behavior, we investigated how long a given hyperpolarization had to be to produce significant effects on Eag2 activation kinetics. For this purpose, we changed the duration of the conditioning prepulses using the same voltage protocol as in Figure 8. The results of these experiments showed that hyperpolarizing prepulses >100 msec are required to obtain significant changes in kinetics, and maximum effects were obtained with prepulses of 3–5 sec (Fig. 7*B*).

We also explored the time required for the channel to recover from a previous membrane depolarization using a standard two-pulse protocol in which we changed the time at rest between two identical depolarizing voltage commands. The results of such experiments demonstrated that previous channel activity strongly influenced the activation rate of Eag2 during a second depolarization (Fig. 9). A previous depolarization increased the rate of activation during the second pulse. Apparently this increase in activation rate is lost slowly; intervals at rest of the order of seconds (>8 sec for the experiment shown in Fig. 9) are required for the channel to fully recover from the effect of the previous depolarization. This property may have important physiological implications by providing a form of short-term plasticity to the cells in which these channels are expressed.

Inactivation

In contrast to most delayed rectifier-type K$^+$ channels, but similar to Eag1, Eag2 currents did not inactivate during long depolarizations. As shown in Figure 5*B*, no inactivation was seen during

depolarizations lasting 7 sec. In fact, little if any inactivation was seen when the cell was tonically depolarized by increasing extracellular potassium levels for >5 min or the cell membrane was clamped to −30 mV for 5 min (data not shown).

Pharmacological properties

A property shared by the members of the Eag family is their relatively low sensitivity to the commonly used K$^+$ channel blockers 4-AP and TEA (Coetzee et al., 1999; Ganetzky et al., 1999). Eag2, like Eag1, is relatively insensitive to 4-AP, a potent blocker of Kv potassium channel family members (Ludwig et al., 1994). In Eag2-injected oocytes, replacement of 20 mM 4-AP for NaCl in the extracellular perfusion had no measurable effect on the macroscopic currents (Table 3).

Eag2 was also weakly sensitive to TEA as compared with other K$^+$ channels. Eag2 was partially blocked by high concentrations of TEA (~75% at 96 mM), and the block was voltage dependent. Dose–response curves for TEA at two different test potentials (−20 and 40 mV) gave IC$_{50}$ values of 12.5 and 19 mM, respectively (Table 3).

Eag2 currents were also blocked by extracellular Ba^{2+} (Fig. 5*G*) and Cs$^+$ ions. Eag2 was much more sensitive to Ba^{2+} than Cs$^+$. The blockade for both was voltage dependent (Table 3). Application of 5 mM Ba^{2+} to the extracellular solution blocked >98% Eag2 currents regardless of voltage (Table 3; also see Fig. 5*G*). Eag2 was insensitive to 1 μM of the antiarrhythmic drug E4031, which is a known blocker of the related Erg members (Shi et al., 1997). Eag1 and the members of the Elk subfamily are also insensitive to this compound (Engeland et al., 1998; Shi et al., 1998; Trudeau et al., 1999).

Modulation

Primary sequence analysis revealed that Eag2 contained many putative phosphorylation sites, including a PKA-PKG site and a cluster of PKC sites at the C terminus of the protein not found in Eag1 (Fig. 1). Interestingly, phorbol 12-myristate 13-acetate (PMA), an activator of PKC, produced a potent dose-dependent block of Eag2 currents. Equivalent concentrations of the weak PKC activator 4α-phorbol 12, 13-didecanoate (4α PDD), however, had little effect (Fig. 10). This suggests that PKC may play a role in the modulation of Eag2 currents.

DISCUSSION

This paper describes the cloning and primary structure of Eag2, a new member of the Eag family of K$^+$ channel pore-forming subunits in mammals. The protein is most similar (74% amino acid identity) to Eag1, the one known member of the Eag subfamily within the mammalian Eag family. Eag2 shares with Eag1, and other members of the Eag family, the same overall structure (Ganetzky et al., 1999). There is strong conservation of the transmembrane core region, of a PAS domain (Morais Cabral et al., 1998) present in the putative intracellular amino end of the protein, and of a cyclic nucleotide binding domain in the putative intracellular carboxyl end following the membrane portion of the protein. Cyclic nucleotides do not affect the function of Eag2 (data not shown) or other mammalian Eag family proteins (Ludwig et al., 1994; Robertson et al., 1996; Frings et al., 1998; Ganetzky et al., 1999). Therefore, if there is a function for this domain in these K$^+$ channel subunits, it remains to be discovered. The strongest sequence divergence between Eag1 and Eag2 is found in the C-terminal area after the cyclic nucleotide binding domain.

Table 3. Pharmacological properties of Eag2 currents

Drug	Effect
TEA	IC$_{50}$ = 19 mM (40 mV)[a]
	IC$_{50}$ = 12.5 mM (−20 mV)[a]
4-AP	No effect at 20 mM
Ba^{2+}	50% blocked by 1 mM (40 mV)[a]
	>98% blocked by 5 mM (at all voltages)
Cs$^+$	50% blocked by 20 mM (40 mV)[a]
	50% blocked by 8 mM (−20 mV)[a]
E4031	No effect at 1 μM

[a]Voltage-dependent block.

Eag2 channels expressed in *Xenopus* oocytes share several unusual properties with Eag1 in this and other heterologous expression systems (Ludwig et al., 1994; Robertson et al., 1996; Terlau et al., 1996; Bijlenga et al., 1998; Frings et al., 1998). If the properties of native neuronal channels containing these proteins are similar to those seen in heterologous expression systems, they could be of considerable physiological significance. These include a characteristic gating behavior with fast and slow components whose contribution to the activation kinetics of the channel depends strongly on the membrane potential before membrane depolarization. Hyperpolarizing prepulse potentials slow down channel opening by increasing the contribution of the slow component, whereas depolarizations decrease this contribution and accelerate the activation kinetics during a subsequent depolarization. The strong dependence of channel activation on prepulse voltage suggests that the kinetics of these channels includes remote closed states that are only occupied significantly at hyperpolarized potentials (Ludwig et al., 1994; Robertson et al., 1996; Terlau et al., 1996). The entry and exit from these states appears to be slow. Thus at rest, after a depolarization, the equilibrium between closed states is reestablished slowly, such that the kinetics of activation of the channels is faster during a second depolarization unless the membrane is maintained at the repolarizing potential for several seconds. The dependence of gating behavior of Eag channels on prepulse potential may contribute a short-term plasticity to the electrical response of neurons expressing these channels.

Both Eag1 and Eag2 channels are also characterized by the lack of inactivation during long depolarizations. Therefore, they can produce steady currents at membrane potentials throughout the voltage range in which the channels activate. The most significant difference between Eag2 and Eag1 currents observed so far is their macroscopic voltage dependence of activation. The midpoints of the conductance–voltage curves of Eag1 and Eag2 differ by ~25–30 mV, and observable opening of Eag2 channels occurs at voltages 40–50 mV more negative (Robertson et al., 1996; Bijlenga et al., 1998). Although both Eag1 and Eag2 currents could limit neuronal excitability, Eag2 will have a greater effect in modulating the resting potential and level of excitability in neurons having resting potentials in the −70 to −90 mV range. Eag2 channels could thus have subthreshold effects on excitability down to the most negative membrane potentials known in neurons.

In this regard, Eag2 currents resemble the M currents (Brown and Adams, 1980; Brown, 1988). Although the activation and deactivation kinetics of Eag2 channels are faster than that of the channels mediating the M current, both show no inactivation and have significant activation at subthreshold voltages. M channels have a midpoint of activation around −35 mV and show signifi-
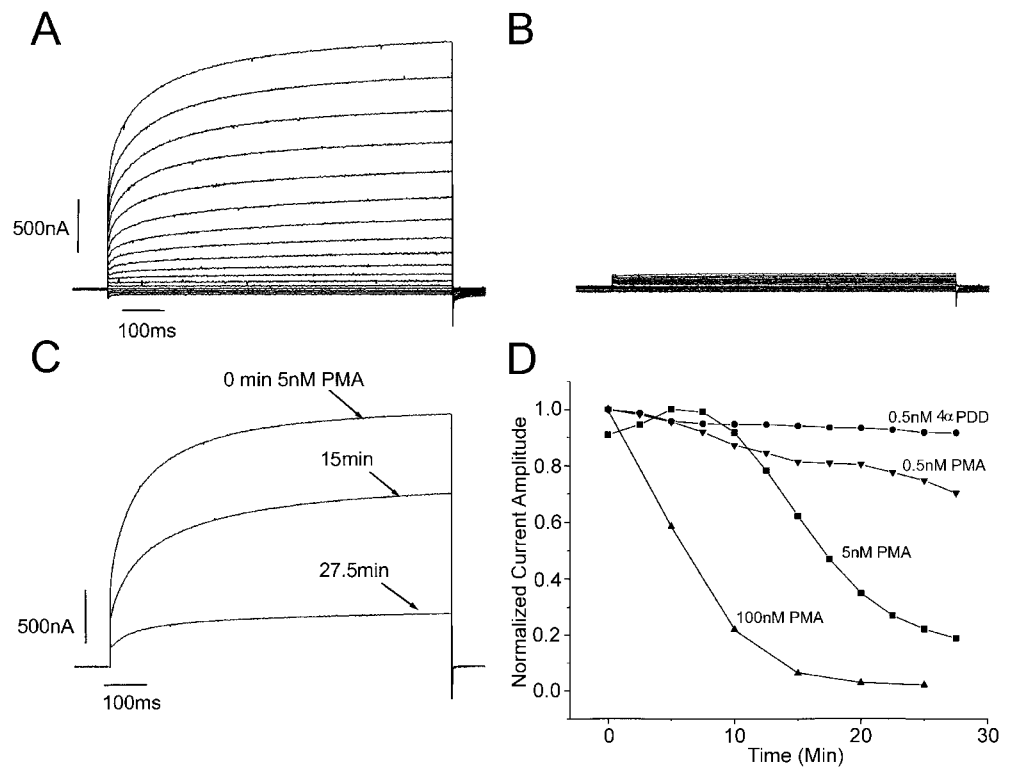
Figure 10. Phorbol esters inhibit Eag2 currents. Currents in an Eag2-injected oocyte in ND96 alone (*A*) or 30 min after application of 100 nM PMA to the extracellular perfusion (*B*) during step depolarizations from −120 to +40 mV in 10 mV increments from a holding potential of −90 mV. *C*, Eag2 currents during test depolarizations to +40 mV from a holding potential of −90 mV at the indicated times after the application of 5 nM PMA to the extracellular solution. *D*, Time course of inhibition of Eag2 steady-state currents from experiments such as the one illustrated in *C* after application of 100 nM (*triangles*), 5 nM (*squares*), 0.5 nM (*inverted triangles*) PMA or 0.5 nM of the less active isomer 4αPDD (*circles*) to the extracellular solution.

cant activation between −60 and −70 mV (Brown, 1988; Wang et al., 1998). Like the channels mediating M currents, Eag2 channels are likely to contribute to the resting potential and the resting membrane conductance and to provide a strong break to membrane potential depolarizing changes, including influencing action potential threshold (Adams and Galvan, 1986; Brown, 1988; Yamada et al., 1989). These effects can be considerable because few conductances are active in the subthreshold voltage range. If Eag2 channels are present in postsynaptic sites, they could influence synaptic responses. In addition, given the fast phase of activation of Eag2 currents, they are even more likely than M currents to be activated significantly during action potentials and to affect their configuration and repetitive firing characteristics.

The molecular basis for the differences in voltage dependence of Eag1 and Eag2 channels remains to be investigated. Point mutations in and around the S4 domain produce large changes in the voltage dependence of Eag and Kv channels (Papazian et al., 1991; Perozo et al., 1994; Schönherr et al., 1999). Another area of interest is the PAS domain. Mutations in this region in Eag1 and HERG (Terlau et al., 1997; Morais Cabral et al., 1998; Chen et al., 1999) have also been shown to produce large changes in voltage dependence. There are several differences between Eag1 and Eag2 in the S3–S5 and PAS domains that might be a potential source for the dramatic shift in voltage dependence observed in Eag2 currents.

Physiological significance

The pattern of expression of Eag2 in brain is also very interesting. We have not yet detected Eag2 outside the nervous system (other than the testes), and in the brain its pattern of expression is among the most selective found for K$^+$ channels so far (Pongs, 1992; Chandy and Gutman, 1995; Coetzee et al., 1999). The expression in the cerebral cortex is particularly interesting and could be of physiological importance. Our data with emulsion

autoradiograms clearly show that Eag2 is predominantly expressed in neurons in cortical layer IV. X-ray autoradiograms show a laminar expression that thickens in areas (granular cortex) where layer IV is more prominent, consistent with this conclusion.

Several types of neurons are in cortical layer IV. These include excitatory local interneurons, including the spiny stellate cells, and the small pyramids or star-pyramids, and inhibitory GABAergic interneurons including multipolar and bipolar cells, which have somewhat larger somatic sizes than the excitatory interneurons. The excitatory interneurons constitute the overwhelming majority of layer IV neurons, outnumbering GABAergic cells approximately 5 or even 10 to 1. There are also a few scattered projecting pyramidal cells such as those that exist in other cortical layers (Jones, 1975; Fairén et al., 1984; Simons and Woolsey, 1984; Keller, 1995). We found through analysis at high magnification of emulsion autoradiograms of sections hybridized to Eag2 probes that a large proportion of the neurons in layer IV are heavily labeled (Fig. 4*D*). Because spiny stellates and star-pyramids represent the overwhelming majority of layer IV neurons, we hypothesize that Eag2 mRNAs are present in these neurons. If Eag2 were expressed *only* in the GABAergic cells, a minority of the cells (1 of 5–10) would have a large density of silver grains, contrary to what we see with Eag2 (Fig. 4*D*). Also, we would not expect to see a uniform band in dark-field images (Fig. 4*A*) but instead scattered signals as seen for Kv3.1 and Kv3.2 K$^+$ channel transcripts (Weiser et al., 1994). Moreover, spiny stellate and star-pyramid neurons occur predominantly in layer IV, unlike known types of GABAergic interneurons (Jones, 1975; Fairén et al., 1984; Simons and Woolsey, 1984). Specific expression of Eag2 in these specialized excitatory interneurons would explain the laminar staining observed in the cortex. However, higher resolution methods, such as immunohistochemistry with Eag2-specific antibodies, will be required to determine with cer-

tainty which populations of cortical layer IV neurons express Eag2.

Layer IV cortical neurons are the main recipients of thalamocortical input (Jones, 1985; Steriade et al., 1990). This input brings to the cortex almost all sensory information. Thalamocortical transmission of sensory inputs is highly regulated depending on the states of vigilance and perhaps other behavioral states of the animal (Steriade et al., 1990, 1993; McCormick, 1992). Modulations at the level of the thalamocortical neuron, mediated by neurotransmitter systems arriving from the brainstem, have been studied extensively (Steriade et al., 1990, 1993; McCormick, 1992). The concentration of Eag2 mRNAs in layer IV neurons and the properties of Eag2 channels in *Xenopus* oocytes, including their modulation by phorbol esters, suggest the intriguing hypothesis that neurotransmitter systems acting on the cortex, including glutamate from the thalamocortical inputs themselves acting on metabotropic receptors, could regulate the transmission of sensory information at the level of the postsynaptic cell.

REFERENCES

Adams PR, Galvan M (1986) Voltage-dependent currents of vertebrate neurons and their role in membrane excitability. Adv Neurol 44:137–170.

Bauer CK, Engeland B, Wulfsen I, Ludwig J, Pongs O, Schwarz JR (1998) RERG is a molecular correlate of the inward-rectifying K current in clonal rat pituitary cells. Receptors Channels 6:19–29.

Baxter DA, Byrne JH (1991) Ionic conductance mechanisms contributing to the electrophysiological properties of neurons. Curr Opin Neurobiol 1:105–112.

Bijlenga P, Occhiodoro T, Liu JH, Bader CR, Bernheim L, Fischer-Lougheed J (1998) An ether-a-go-go K+ current, Ih-eag, contributes to the hyperpolarization of human fusion-competent myoblasts. J Physiol (Lond) 512:317–323.

Broillet M-C, Firestein S (1999) Cyclic nucleotide-gated channels. Ann NY Acad Sci 868:730–740.

Brown DA (1988) M currents. In: Ion channels (Narahashi ET, ed), pp 55–94. New York: Plenum.

Brown DA, Adams PR (1980) Muscarinic suppression of a novel voltage-sensitive K+ current in a vertebrate neurone. Nature 283:673–676.

Chandy KG, Gutman GA (1995) Voltage gated channels. In: Handbook of receptors and channels: ligand-gated and voltage-gated ion channels (North AP, ed), pp 1–71. Boca Raton, FL: CRC.

Chen J, Zou A, Splawski I, Keating MT, Sanguinetti MC (1999) Long QT syndrome-associated mutations in the Per-Arnt-Sim (PAS) domain of HERG potassium channels accelerate channel deactivation. J Biol Chem 274:10113–10118.

Chomczynski P, Sacchi N (1987) Single-step method of RNA isolation by acid guanidinium thiocyanate-phenol-chloroform extraction. Anal Biochem 162:156–159.

Coetzee W, Amarillo Y, Chiu J, Chow A, Lau D, McCormack T, Moreno H, Nadal MS, Ozaita A, Pountney D, Saganich M, Vega-Saenz de Miera E, Rudy B (1999) Molecular diversity of K$^+$ channels. Ann NY Acad Sci 868:233–285.

Curran ME, Splawski I, Timothy KW, Vincent GM, Green ED, Keating MT (1995) A molecular basis for cardiac arrhythmia: HERG mutations cause long QT syndrome. Cell 80:795–803.

Doyle DA, Morais Cabral J, Pfuetzner RA, Kuo A, Gulbis JM, Cohen SL, Chait BT, MacKinnon R (1998) The structure of the potassium channel: molecular basis of K+ conduction and selectivity. Science 280:69–77.

Drysdale R, Warmke J, Kreber R, Ganetzky B (1991) Molecular characterization of eag: a gene affecting potassium channels in *Drosophila melanogaster*. Genetics 127:497–505.

Engeland B, Neu A, Ludwig J, Roeper J, Pongs O (1998) Cloning and functional expression of rat ether-a-go-go-like K+ channel genes. J Physiol (Lond) 513:647–654.

Fairén A, DeFilipe J, Regidor J (1984) Non-pyramidal neurons: general account. In: Cerebral cortex (Peters A, Jones EG, eds), pp 201–254. New York: Plenum.

Frings S, Brull N, Dzeja C, Angele A, Hagen V, Kaupp UB, Baumann A (1998) Characterization of ether-a-go-go channels present in photoreceptors reveals similarity to IKx, a K+ current in rod inner segments. J Gen Physiol 111:583–599.

Ganetzky B, Robertson AG, Wilson FG, Trudeau MC, Titus SA (1999) The eag family of K$^+$ channels in *Drosophila* and mammals. Ann NY Acad Sci 868:356–369.

Hahn ME, Karchner SI, Shapiro MA, Perera SA (1997) Molecular evolution of two vertebrate aryl hydrocarbon (dioxin) receptors (AHR1 and AHR2) and the PAS family. Proc Natl Acad Sci USA 94:13743–13748.

Hartmann HA, Kirsch GE, Drewe JA, Taglialatela M, Joho RH, Brown AM (1991) Exchange of conduction pathways between two related K+ channels. Science 251:942–944.

Hille B (1992) Ionic channels of excitable membranes. Sunderland, MA: Sinauer.

Hoshi N, Takahashi H, Shahidullah M, Yokoyama S, Higashida H (1998) KCR1, a membrane protein that facilitates functional expression of non-inactivating K+ currents associates with rat EAG voltage-dependent K+ channels. J Biol Chem 273:23080–23085.

Iverson LE, Rudy B (1990) The role of the divergent amino and carboxyl domains on the inactivation properties of potassium channels derived from the Shaker gene of *Drosophila*. J Neurosci 10:2903–2916.

Jan LY, Jan YN (1997) Cloned potassium channels from eukaryotes and prokaryotes. Annu Rev Neurosci 20:91–123.

Jones EG (1975) Varieties and distribution of non-pyramidal cells in the somatic sensory cortex of the squirrel monkey. J Comp Neurol 160:205–267.

Jones EG (1985) The thalamus. New York: Plenum.

Kaczmareck KL, Levitan IB (1987) Neuromodulation: the biochemical control of neuronal excitability. New York: Oxford UP.

Keller A (1995) Synaptic organization of the barrel cortex. In: Cerebral cortex (Jones E, Diamond IT, eds), pp 221–262. New York: Plenum.

Klein M, Camardo J, Kandel ER (1982) Serotonin modulates a specific potassium current in the sensory neurons that show presynaptic facilitation in *Aplysia*. Proc Natl Acad Sci USA 79:5713–5717.

Latorre R, Oberhauser A, Labarca P, Alvarez O (1989) Varieties of calcium-activated potassium channels. Annu Rev Physiol 51:385–399.

Levitan IB (1988) Modulation of ion channels in neurons and other cells. Annu Rev Neurosci 11:119–136.

Liman ER, Tytgat J, Hess P (1992) Subunit stoichiometry of a mammalian K+ channel determined by construction of multimeric cDNAs. Neuron 9:861–871.

Llinas RR (1988) The intrinsic electrophysiological properties of mammalian neurons: insights into central nervous system function. Science 242:1654–1664.

Ludwig J, Terlau H, Wunder F, Bruggemann A, Pardo LA, Marquardt A, Stuhmer W, Pongs O (1994) Functional expression of a rat homologue of the voltage gated ether a go-go potassium channel reveals differences in selectivity and activation kinetics between the *Drosophila* channel and its mammalian counterpart. EMBO J 13:4451–4458.

Ludwig J, Owen D, Pongs O (1997) Carboxy-terminal domain mediates assembly of the voltage-gated rat ether-a-go-go potassium channel. EMBO J 16:6337–6345.

MacKinnon R, Yellen G (1990) Mutations affecting TEA blockade and ion permeation in voltage- activated K+ channels. Science 250:276–279.

McCormick DA (1990) Membrane properties and neurotransmitter actions. In: The synaptic organization of the brain (Shepherd GM, ed), pp 32–66. New York: Oxford UP.

McCormick DA (1992) Neurotransmitter actions in the thalamus and cerebral cortex and their role in neuromodulation of thalamocortical activity. Prog Neurobiol 39:337–388.

Morais Cabral JH, Lee A, Cohen SL, Chait BT, Li M, Mackinnon R (1998) Crystal structure and functional analysis of the HERG potassium channel N terminus: a eukaryotic PAS domain. Cell 95:649–655.

North RA (1989) Drug receptors and the inhibition of nerve cells. Br J Pharmacol 98:13–28.

Papazian DM, Timpe LC, Jan YN, Jan LY (1991) Alteration of voltage-dependence of Shaker potassium channel by mutations in the S4 sequence. Nature 349:305–310.

Perozo E, Santacruz-Toloza L, Stefani E, Bezanilla F, Papazian DM (1994) S4 mutations alter gating currents of Shaker K channels. Biophys J 66:345–354.

Pongs O (1992) Molecular biology of voltage-dependent potassium channels. Physiol Rev 72:S69–88.

Ponting CP, Aravind L (1997) PAS: a multifunctional domain family comes to light. Curr Biol 7:R674–677.

Reppert SM (1998) A clockwork explosion! Neuron 21:1–4.

Robertson GA, Warmke JM, Ganetzky B (1996) Potassium currents expressed from *Drosophila* and mouse eag cDNAs in *Xenopus* oocytes. Neuropharmacology 35:841–850.

Rudy B (1988) Diversity and ubiquity of K channels. Neuroscience 25:729–749.

Rudy B, Hoger JH, Lester HA, Davidson N (1988) At least two mRNA species contribute to the properties of rat brain A-type potassium channels expressed in *Xenopus* oocytes. Neuron 1:649–658.

Rudy B, Chow A, Lau D, Amarillo Y, Ozaita A, Saganich M, Moreno H, Nadal MS, Hernandez-Pineda R, Hernandez-Cruz A, McIntosh P, Erisir A, Leonard C, Vega-Saenz de Miera E (1999) Contributions of Kv3 channels to neuronal excitability. Ann NY Acad Sci 868:304–343.

Sambrook J, Fritsch E, Maniatis T (1989) Molecular cloning: a laboratory manual, Ed 2. Cold Spring Harbor, NY: Cold Spring Harbor Laboratory.

Sanguinetti MC (1999) Dysfunction of delayed rectifier potassium channels in an inherited cardiac arrhythmia. Ann NY Acad Sci 868:406–411.

Santoro B, Tibbs GR (1999) The HCN gene family: molecular basis of the hyperpolarization-activated pacemaker channels. Ann NY Acad Sci 868:741–764.

Sassone-Corsi P (1998) Molecular clocks: mastering time by gene regulation. Nature 392:871–874.

Schönherr R, Hehl S, Terlau H, Baumann A, Heinemann SH (1999) Individual subunits contribute independently to slow gating of bovine EAG potassium channels. J Biol Chem 274:5362–5369.

Shi W, Wymore RS, Wang HS, Pan Z, Cohen IS, McKinnon D, Dixon JE (1997) Identification of two nervous system-specific members of the erg potassium channel gene family. J Neurosci 17:9423–9432.

Shi W, Wang HS, Pan Z, Wymore RS, Cohen IS, McKinnon D, Dixon JE (1998) Cloning of a mammalian elk potassium channel gene and EAG mRNA distribution in rat sympathetic ganglia. J Physiol (Lond) 511:675–682.

Siegelbaum SA, Camardo JS, Kandel ER (1982) Serotonin and cyclic AMP close single K+ channels in *Aplysia* sensory neurones. Nature 299:413–417.

Sigworth FJ (1994) Voltage gating of ion channels. Q Rev Biophys 27:1–40.

Simons DJ, Woolsey TA (1984) Morphology of Golgi-Cox-impregnated barrel neurons in rat SmI cortex. J Comp Neurol 230:119–132.

Steriade M, Jones EG, Llinas RR (1990) Thalamic oscillations and signaling. New York: Wiley.

Steriade M, McCormick DA, Sejnowski TJ (1993) Thalamocortical oscillations in the sleeping and aroused brain. Science 262:679–685.

Stone DM, Wessel T, Joh TH, Baker H (1990) Decrease in tyrosine hydroxylase, but not aromatic L-amino acid decarboxylase, messenger RNA in rat olfactory bulb following neonatal, unilateral odor deprivation. Brain Res Mol Brain Res 8:291–300.

Terlau H, Ludwig J, Steffan R, Pongs O, Stuhmer W, Heinemann SH (1996) Extracellular Mg^{2+} regulates activation of rat eag potassium channel. Pflügers Arch 432:301–312.

Terlau H, Heinemann SH, Stuhmer W, Pongs O, Ludwig J (1997) Amino terminal-dependent gating of the potassium channel rat eag is compensated by a mutation in the S4 segment. J Physiol (Lond) 502:537–543.

Thomson J, Higgins D, Gibson T (1994) CLUSTAL W: improving the sensitivity of progressive multiple sequence alignment through sequence weighing, position specific gap penalties, and weight matrix choice. Nucleic Acids Res 22:4673–4680.

Trudeau MC, Warmke JW, Ganetzky B, Robertson GA (1995) HERG, a human inward rectifier in the voltage-gated potassium channel family. Science 269:92–95.

Trudeau MC, Titus SA, Branchaw JL, Ganetzky B, Robertson GA (1999) Functional analysis of a mouse brain Elk-type K+ channel. J Neurosci 19:2906–2618.

Wang HS, Pan Z, Shi W, Brown BS, Wymore RS, Cohen IS, Dixon JE, McKinnon D (1998) KCNQ2 and KCNQ3 potassium channel subunits: molecular correlates of the M-channel. Science 282:1890–1893.

Warmke JW, Ganetzky B (1994) A family of potassium channel genes related to eag in *Drosophila* and mammals. Proc Natl Acad Sci USA 91:3438–3442.

Warmke J, Drysdale R, Ganetzky B (1991) A distinct potassium channel polypeptide encoded by the *Drosophila* eag locus. Science 252:1560–1562.

Weiser M, Vega-Saenz de Miera E, Kentros C, Moreno H, Franzen L, Hillman D, Baker H, Rudy B (1994) Differential expression of Shaw-related K+ channels in the rat central nervous system. J Neurosci 14:949–972.

Yamada WM, Koch C, Adams PR (1989) Methods in neuronal modeling (Koch C, Segev I, eds), pp 97–133. Cambridge, MA: Bradford.

Yool AJ, Schwarz TL (1991) Alteration of ionic selectivity of a K+ channel by mutation of the H5 region. Nature 349:700–704.

Young SH, Moore JW (1981) Potassium ion currents in the crayfish giant axon. Dynamic characteristics. Biophys J 36:723–733.

Zhulin IB, Taylor BL, Dixon R (1997) PAS domain S-boxes in archaea, bacteria and sensors for oxygen and redox. Trends Biochem Sci 22:331–333.